

**OCEAN RESOURCES INVESTIGATION
IN THE SEA AREA OF CCOP/SOPAC
REPORT ON THE JOINT BASIC STUDY
FOR THE DEVELOPMENT OF RESOURCES**

(VOLUME 4)

SEA AREA OF TUVALU

February 1989

**JAPAN INTERNATIONAL COOPERATION AGENCY
METAL MINING AGENCY OF JAPAN**

MPN
CR 6
89-34

2387

JICA LIBRARY



1078959(2)

**OCEAN RESOURCES INVESTIGATION
IN THE SEA AREA OF CCOP/SOPAC
REPORT ON THE JOINT BASIC STUDY
FOR THE DEVELOPMENT OF RESOURCES**

(VOLUME 4)

SEA AREA OF TUVALU

February 1989

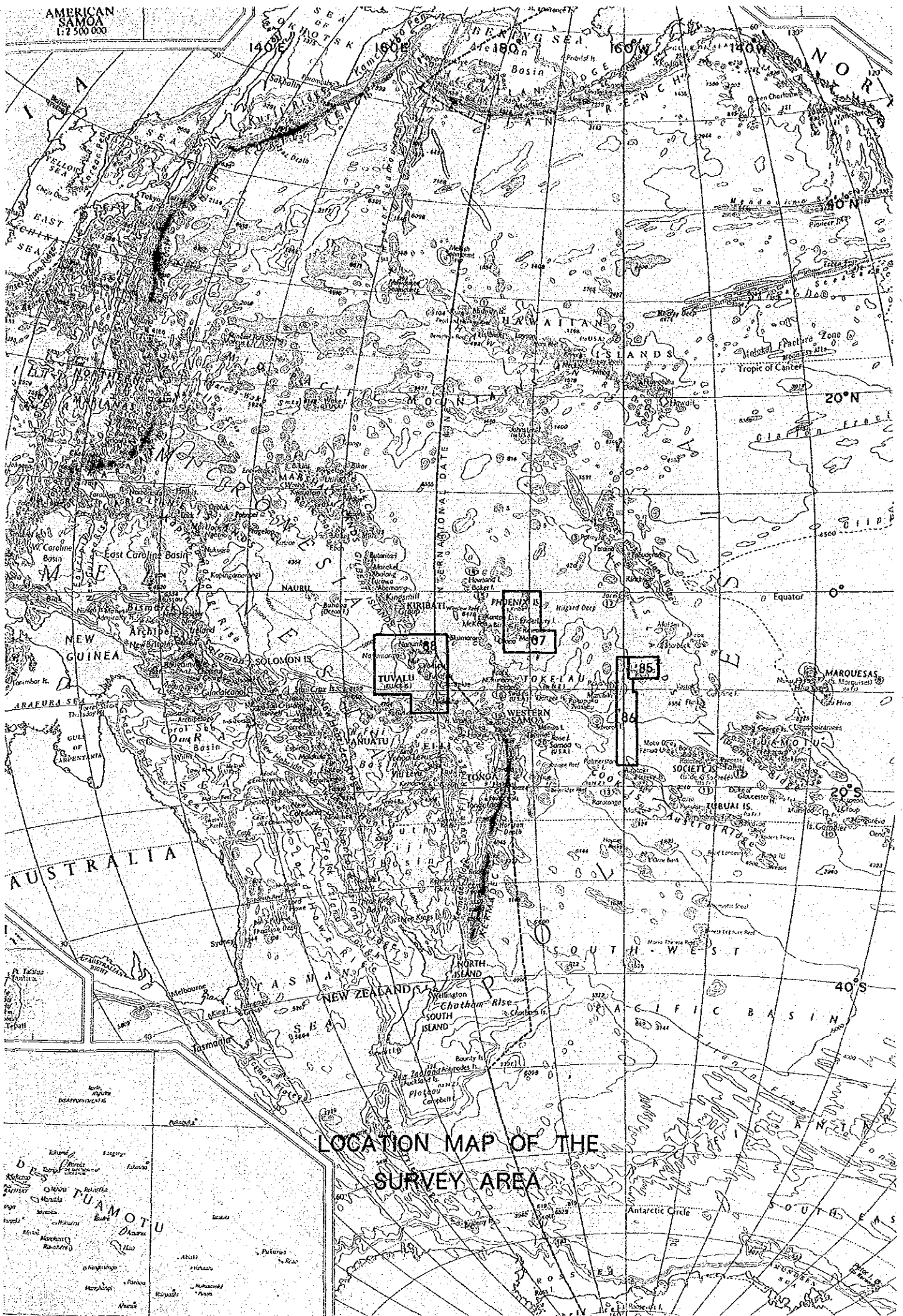
**JAPAN INTERNATIONAL COOPERATION AGENCY
METAL MINING AGENCY OF JAPAN**

MPN
CR (5)
89-34



国際協力事業団

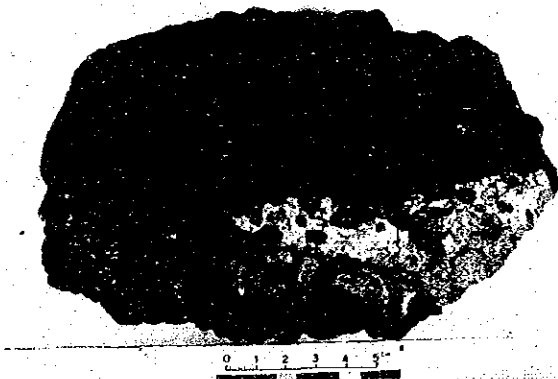
20387



LOCATION MAP OF THE
SURVEY AREA



Cobalt crust exposure with thin foraminifera sands cover at western slope of SB08 - seamount of 1,500 m water depth. Botryoidal surface structure denotes certain thickness of crust same as dredged samples with upto about 2 cm nearby. (No. FDC06-41)



Section of cobalt crust with maximum thickness (6.5 cm), single layer structure, and hyaloclastic substrate with phosphoritic matrix.

Grade: Co 0.93%, Ni 0.64%, Cu 0.07%, Mn 25.85%, Fe 15.20%, H₂O 35.23%.

(No. SB08AD08-A)

Representative Occurrence of Cobalt Crust in the Surveyed Area.

PREFACE

In response to the request of the Committee for Co-ordination of Joint Prospecting for Mineral Resources in the South Pacific Offshore Areas (CCOP/SOPAC), the Government of Japan decided to conduct studies relating to mineral prospecting such as marine geological studies in order to assess the mineral resources potential on the deep ocean floor of the offshore region of the CCOP/SOPAC member countries and consigned implementation of the survey to the Japan International Cooperation Agency (JICA).


Considering the technical nature of the geological and mineral prospecting studies, the JICA commissioned the Metal Mining Agency of Japan (MMAJ) to execute the survey.

The survey will be undertaken over a five year period starting from the financial year of 1985. In 1988 the fourth year, the MMAJ, taking the Hakurei Maru No.2, a research vessel especially commissioned for prospecting mineral resources on the deep ocean bottom, to the sites of the survey from August 26, 1988 until October 26, 1988, and completed the research activities on schedule.

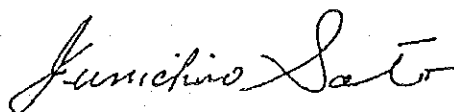
The present report sums up the results of the survey accomplished in the fourth year.

We wish to tender our sincere thanks to all the persons concerned, especially of the Secretariat of CCOP/SOPAC, the Government of Tuvalu and also the Ministry of Foreign Affairs, the Ministry of International Trade and Industry, and the Japanese Embassy in Fiji that willingly collaborated with us.

February, 1989



Japan International Cooperation Agency
President Kensuke YANAGIYA



Metal Mining Agency of Japan
President Junichiro SATO

ABSTRACT

We continued this year, the survey in the waters of Tuvalu, marine area of approximately 690,000 km². The duration of the survey cruise was from 26th, August to 26th, October, of which 43 days was in Tuvalu waters. This was carried out as the fourth year survey of the joint basic study for resources development in the CCOP/SOPAC region. The survey was conducted with a view to assess the resources potential of manganese nodules and cobalt rich crust (cobalt crust or crust in short).

The methods of the survey for the manganese nodules are as follows:

- Topographic and geological survey by acoustic methods,
- Sampling by the sampler FG (Free Fall Grab), (primary survey: 24 stations).

The methods of the survey for cobalt crust are as follows:

- Topographic survey and dredging (89 stations) on the selected eight seamounts (including 2 atolls),
- Observation and photography by FDC (5 seamounts, 37.2 miles in total length).

The abundance of manganese nodules was not as good as expected and good cobalt crusts were confirmed in only a part of the seamounts investigated.

The sea-floor topography of the survey area is divided into the western plain and the eastern quasi-plain by the Ellice Island Chain which is developed in the central part. The water depth of the area is the order of 5,200~5,600 m. In the eastern part, topography with ENE-WSW is dominant and the relief is high. There are approximately 25 seamounts in the area, of which nine are atolls and three are banks. Other seamounts are submerged with peaks of varying water depth.

The geology of the area consists essentially of basalt basement with overlying unconsolidated sediments. The basalts are lavas and hyaloclastites. The unconsolidated sediments are 10~60 m thick in plains and quasi-plains and less than several meters in mountainous parts. Brown clay is predominant in the sediments deeper than 4,900 m and calcareous clay is distributed on the sea-floor less than 4,900 m deep.

The distribution of manganese nodules is generally sparse and discontinuous. Relatively high abundance area (>7.5 kg/m²) was observed in only several stations in the northeastern part of the survey area. Arithmetic average of all sampling stations is 2.74 kg/m². The arithmetic average of major metal contents of all sampling stations are 0.54% Ni, 0.47% Cu, 0.20% Co, 17.01% Mn, and 12.73% Fe. The manganese nodules are mostly pebbly and they belong morphologically to the S type (smooth type). Significant morphological variation of the nodules was not observed in the survey area.

As for the cobalt crust, the development of crusts was confirmed in all eight seamounts, but they are very thin. There was only one seamount where the average thickness of all stations exceeded 1 cm.

Cobalt crusts occur throughout survey area in water depth from 810~2,930 m. The total amount of samples collected, including substrates was 2,695 kg. The mode of occurrence and characteristics of the crusts are as follows.

- a) Confirmed depth of crust development is 900~2,800 m, but the upper and the lower limit of the depth is expected to extend beyond present findings.
- b) The mode of occurrence are crust, slab, block, cobble and nodule in shape.
- c) The inner structures of the crusts have various types, such as single layer, double layers, triple layers, and it generally becomes more compact in the lower layer (inner core) adjacent to the substrate.
- d) The major constituent mineral is δ -MnO₂, and 10Å manganite is often associated in the inner core.
- e) The host rocks are basalt, limestone, and phosphorite.
- f) The average crust thickness of all 74 sampled stations is 0.3 cm, the maximum is about 6.5 cm.
- g) Coverage of crusts on the peaks of the seamounts is different from that on the banks. It is generally higher on the peaks and the upper slopes of seamounts.
- h) The average grade of crusts from the 43 sampling points used for analysis and data processing are 0.78% Co, 0.50% Ni, 0.09% Cu, 21.86% Mn, and 18.03% Fe.
- i) Confirmed characteristics of the Mn/Fe ratio of the crusts of this area is 1.21 which is considerably lower than those of the seamounts distributed in the Central Pacific Ocean.

By this survey, we obtained the general information regarding the occurrence of the deep sea mineral resources in the survey area. But the possibility of locating topographically favourable zones with high manganese nodule abundance in the future is very small. On the other hand, the submerged seamounts of the northeastern part of the area appear promising for locating significant amount of cobalt crust thicker than 1 cm.

CONTENTS

	Page
Preface	
Abstract	
Chapter 1. Main Points of the Survey	
1-1 Title of the Survey	1
1-2 Objectives of the Survey	1
1-3 Sea Areas of the Survey	1
1-4 Period of the Survey	1
1-5 Participants of the Survey	3
1-6 Apparatus and Equipment for the Survey	5
1-7 Records of the Survey	6
Chapter 2. Survey Methods	
2-1 Manganese Nodules	11
1) Survey Procedures	11
2) Numbering Track Lines, Sampling Stations and Sampling Points ...	11
3) Ship Positioning	13
4) Sea-Floor Topography	13
5) Surficial Sediments	13
6) Manganese Nodule Survey by MFES	14
7) Sampling and Sea Bottom Observation by Deep-sea Camera	14
8) Processing, Analysis and Storage of Samples	17
9) Processing and Analysis of the Survey Data	17
2-2 Cobalt Crusts	21
1) Survey Procedures	21
2) Numbering Track Lines, Sampling Stations and Sampling Points ...	21
3) Ship Positioning	21
4) Sea-Floor Topography	22
5) Surficial Sediments	22
6) Sampling	22
7) Processing, Analysis and Storage of Samples	22
8) Sea Bottom Observation by FDC	22
9) Processing and Analysis of Survey Data	23

Chapter 3. Results of the Survey (Manganese Nodules)

3-1	Sea-Floor Topography	25
	1) Regional Topography	25
	2) Classification of Sea-Floor Topography	25
3-2	Surficial Sediments	29
	1) Classification of SBP Records	29
	2) Distribution of SBP Types	31
	3) Distribution of the Upper Transparent Layers	32
3-3	Bottom Materials	33
	1) Classification	33
	2) Distribution and Properties	33
	3) Mineral Composition	36
	4) Chemical Composition	39
	5) Authigenic Minerals	41
	6) Carbonate Compensation Depth (CCD)	41
	7) Paleontological Considerations	43
3-4	MFES Survey of Manganese Nodules	60
	1) Effect of Topography and Sediments	60
	2) Buried Manganese Nodules	62
	3) Estimation of Manganese Nodule Distribution by MFES	63
3-5	Modes of Manganese Nodule Occurrences	65
	1) Classification and Properties	65
	2) Abundance and Occurrence	71
	3) Chemical Properties	79
	4) Mineralogy	88
	5) Sea-Floor Conditions and Abundance	92
	6) Total Metal Content	96
3-6	Discussions	98

Chapter 4. Results of the Survey (Cobalt Crust)

4-1	Seamount Topography	101
	1) Classification	101
	2) Topographic Features	105
4-2	Seamount Geology	111
	1) Geology	111
	2) Description of Substrates	113
	3) Age Determination	113

4-3	Mode of Cobalt Crust Occurrences	121
	1) Distribution and Occurrence	121
	2) FDC Survey	133
	3) Chemical Properties	142
	4) Mineralogy	153
4-4	Discussions	159

Chapter 5. Summary

5-1	Methods of the Survey	161
5-2	Topography and Geology	161
5-3	Mode of Manganese Nodule Occurrence	162
5-4	Mode of Cobalt Crust Occurrence	163

[References]

[Appendix]

List of the Survey Results

1. Manganese Nodules (1) - (4)
2. Cobalt Crusts (1) - (6)

Weather and Sea-state Data

Annexed Figures (1) - (18)

(List of Inserted Figures)

Figure 1-1	Location Map of the Survey Area	2
Figure 2-1	Location Map of Survey Stations, Seamounts and Others	12
Figure 2-2	Explanation on Setting Order of Three Samplers at a Sampling Station	14
Figure 2-3	Processing and Assaying Flowsheet of Samples (1) and (2)	15
Figure 2-4	Acoustic Sounding and Processing Flowsheet (Manganese Nodule)	20
Figure 2-5	Acoustic Sounding and Processing Flowsheet (Cobalt Crust)	24
Figure 3-1-1	General Sea Floor Topography (Plan)	26
Figure 3-2-1	Classification of SBP Records	30
Figure 3-3-1	Distribution of Bottom Materials	34
Figure 3-3-2	Smear Slide Photos of Bottom Sediments	35
Figure 3-3-3	Typical X-ray Diffraction Patterns of Bottom Sediments	38
Figure 3-3-4	Typical X-ray Diffraction Patterns of Authigenic Minerals	42
Figure 3-3-5	Species of the Typical Radiolarian Fossils (1) and (2)	46
Figure 3-3-6	Species of the Typical Foraminifera Fossils (1) and (2)	56
Figure 3-4-1	Relation Between MFES Intensity and Abundance of Manganese Nodules	61
Figure 3-4-2	Distribution of Embedded Type Manganese Nodules	62
Figure 3-4-3	Influence of Embedded Type Manganese Nodules on MFES Measurement	63
Figure 3-5-1	Morphology of Manganese Nodules (1) and (2)	66
Figure 3-5-2	Morphology and Sampling Weight of Manganese Nodules	68
Figure 3-5-3	Size and Sampling Weight of Manganese Nodules	69
Figure 3-5-4	Morphology Distribution of Manganese Nodules	71
Figure 3-5-5	Size Distribution of Manganese Nodules	72
Figure 3-5-6	Relation between Size and Morphology	73
Figure 3-5-7	Relation between Local Topography and Morphology	74
Figure 3-5-8	Relation between SBP Type and Morphology	75
Figure 3-5-9	Relation between Upper Transparent Layer Thickness and Morphology	76
Figure 3-5-10	Relation between Bottom Sediments and Morphology	77

Figure 3-5-11	Relation between Morphology and Abundance	78
Figure 3-5-12	Frequency Distribution of Five Principal Chemical Components	80
Figure 3-5-13	Scatter Distribution Diagram among Respective Components	81
Figure 3-5-14	Relation between Each Five Principal Chemical Components and Water Depth	85
Figure 3-5-15	X-ray Diffraction Pattern of Manganese Nodules	91
Figure 3-5-16	Macro-Photo and Microscopic Photos of Polished Thin Section of Manganese Nodules	93
Figure 3-5-17	Relation between Macroscopic Topography and Abundance of Manganese Nodules	94
Figure 3-5-18	Relation between Microscopic Topography and Abundance of Manganese Nodules	94
Figure 3-5-19	Relation between SBP Type and Abundance of Manganese Nodules	95
Figure 3-5-20	Relation between Upper Transparent Layer Thickness and Abundance of Manganese Nodules	95
Figure 4-1-1	SBP Profile of Seamounts	106
Figure 4-1-2	Bird's-eye View of Seamounts	107
Figure 4-2-1	Photos of Representative Rocks	117
Figure 4-2-2	Microscopic Photos of Substrates of Cobalt Crusts	119
Figure 4-3-1	Representative Cobalt Crust Types (On Board)	127
Figure 4-3-2	Representative Cobalt Crust Types (Section)	129
Figure 4-3-3	Frequency Distribution of Thickness of Cobalt Crusts	131
Figure 4-3-4	Modified Distribution of Cobalt Crusts along FDC-Survey Line (1) ~ (5)	134
Figure 4-3-5	Sea Bottom Pictures by FDC Survey	139
Figure 4-3-6	Frequency Distribution of Major Five Chemical Components	150
Figure 4-3-7	Correlative Diagram among Major Chemical Components (1) and (2)	151
Figure 4-3-8	X-ray Diffraction Patterns of Cobalt Crusts	155
Figure 4-3-9	Reflective Microscopic Photos of Cobalt Crusts	156
Figure 4-3-10	EPMA Figures of Cobalt Crusts	157

(List of Inserted Tables)

Table 1-1	Apparatus and Equipment for the Survey	5
Table 1-2	List of Survey Achievements (1) ~ (3)	6
Table 1-3	Records of Survey Schedule	9
Table 3-1-1	Classification of Sea Floor Topography	27
Table 3-3-1	Classification Standards of Bottom Materials	33
Table 3-3-2	Sampling Ratio of Bottom Materials	34
Table 3-3-3	Results of X-ray Diffraction Analysis of Bottom Materials ...	37
Table 3-3-4	Chemical Composition of the Bottom Materials	40
Table 3-3-5	Corelations among Chemical Components of Bottom Materials	41
Table 3-3-6	Results of X-ray Diffraction Analysis of Authigenic Minerals	42
Table 3-3-7	List of Radiolarian Fossiles (1) and (2)	44
Table 3-3-8	List of Foraminifera Fossiles	53
Table 3-5-1	Physical Properties Associated with Morphology of Manganese Nodules	70
Table 3-5-2	Chemical Properties of Manganese Nodules	82
Table 3-5-3	Morphology and Chemical Properties of Manganese Nodules	84
Table 3-5-4	Size and Chemical Properties of Manganese Nodules	86
Table 3-5-5	Sea Floor Topography and Chemical Properties of Manganese Nodules	87
Table 3-5-6	Bottom Sediments and Chemical Properties of Manganese Nodules	87
Table 3-5-7	Total and Minor Element Analysis of Manganese Nodules	89
Table 3-5-8	Result of X-ray Diffraction Analysis of Manganese Nodules	90
Table 4-1-1	Classification of Topographic Type of Seamount	101
Table 4-1-2	Classification of Topography of Seamount	101
Table 4-1-3	Topographic Feature of Individul Seamount	102
Table 4-1-4	Topographic Feature of Individual Seamount (1) ~ (3)	103
Table 4-2-1	Geology of Individual Seamount	112
Table 4-2-2	Description of Substrates of Cobalt Crusts (1) and (2)	114

Table 4-2-3	Mineral Assemblage of Substrates	116
Table 4-2-4	Chemical Composition of Substrates	120
Table 4-2-5	Result of Age Determination of Substrate	113
Table 4-3-1	Classification of Types of Cobalt Crusts	122
Table 4-3-2	Occurrences of Cobalt Crusts at Individual Seamount (1) ~ (3)	123
Table 4-3-3	Average Thickness of Cobalt Crust at Each Seamount	131
Table 4-3-4	Bearing Rates of Different Rock Types in Each Crust Types	133
Table 4-3-5	FDC Observation of Cobalt Crust at Each Seamount	141
Table 4-3-6	Cobalt Crust Coverage along FDC Survey Lines	142
Table 4-3-7	Average Grade of Cobalt Crusts at Each Seamount	144
Table 4-3-8	Cobalt Crust Grade and Topographic Position of Seamount ...	144
Table 4-3-9	Cobalt Crust Grade and Surface Structure	145
Table 4-3-10	Cobalt Crust Grade and Substrates	145
Table 4-3-11	Cobalt Crust Grade from Different Layer	146
Table 4-3-12	Cobalt Crust Grade and Types	146
Table 4-3-13	Cobalt Crust Grade and Water Depth	146
Table 4-3-14	Analysis of Total and Minor Element of Cobalt Crust	147
Table 4-3-15	Analysis of Total and Minor Element from Different Layer of Cobalt Crust	148
Table 4-3-16	Mutual Relations among Major Chemical Composition of Cobalt Crust	149
Table 4-3-17	Comparison of Cobalt Crust Compositions	149
Table 4-3-18	Mineral Assemblage of Cobalt Crust, by X-ray Diffraction Analysis	154
Table 5-1	General Occurrences of Cobalt Crusts at Individual Seamount (1) and (2)	164

(List of Annexed Figures)

- Annexed Figure 1 Trackline Map
- Annexed Figure 2 Positions of Sampling Points
- Annexed Figure 3 Sea Floor Topography
- Annexed Figure 4 Distribution of SBP Types
- Annexed Figure 5 Acoustic Thickness of Upper Transparent Layers
Obtained by SBP Survey
- Annexed Figure 6 Estimated Abundance Map of Manganese Nodules
by MFES
- Annexed Figure 7 Abundance Map of Manganese Nodules
- Annexed Figure 8 Ni Grade Map of Manganese Nodules
- Annexed Figure 9 Cu Grade Map of Manganese Nodules
- Annexed Figure 10 Co Grade Map of Manganese Nodules
- Annexed Figure 11 Mn Grade Map of Manganese Nodules
- Annexed Figure 12 Fe Grade Map of Manganese Nodules
- Annexed Figure 13 Ni Metal Quantity Map
- Annexed Figure 14 Cu Metal Quantity Map
- Annexed Figure 15 Co Metal Quantity Map
- Annexed Figure 16 Trackline Maps of Individual Seamount
- Annexed Figure 17 Topographic Plans and Sections of Individual Seamount
(1) ~ (8)
- Annexed Figure 18 Geology and Distribution of Cobalt Crusts of Individual
Seamount (1) ~ (8)

Chapter 1. Main Points of the Survey

1-1 Title of the Survey

The 1988 financial year - Joint Basic Study for the Development of Mineral Resources in the Exclusive Economic Zone of Tuvalu.

1-2 Objectives of the Survey

The objective of the survey is to assess the potential of deep sea mineral resources in the marine areas of the CCOP/SOPAC region.

1-3 Sea Areas of the Survey

Pursuant to the Cooperative Study Programme and its Scope of Work relating to the deep sea mineral resources in the economic waters of the member countries of CCOP/SOPAC, concluded in July 18, 1985 between the executing agency of Japan and CCOP/SOPAC, the marine areas contained in a polygon (area: approximately 678,800 km², Fig. 1-1) bounded by geodesic lines drawn between coordinates listed below were designated as the survey areas.

	Latitude	Longitude
1	4°00' S	174°00' E
2	10°00' S	174°00' E
3	10°00' S	178°00' E
4	12°00' S	178°00' E
5	12°00' S	178°00' W
6	4°00' S	178°00' W
1	4°00' S	174°00' E

1-4 Period of the Survey

Survey: August 26, 1988 - October 26, 1988 (62 days)

Analysis: October 27, 1988 - February 10, 1989

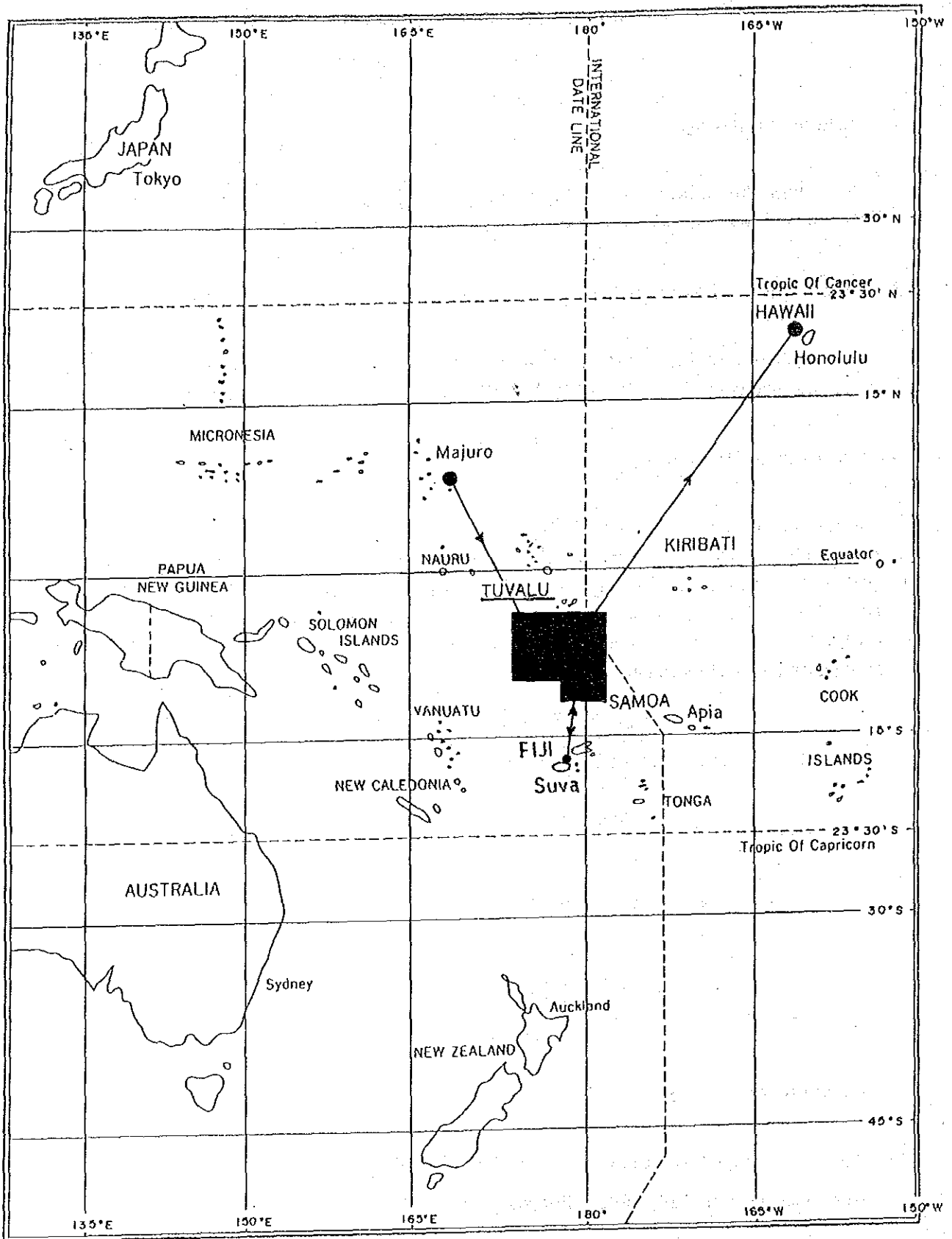


Figure 1-1 Location Map of the Survey Area

1-5 Participants in the Survey

Japanese side

Supervisors at the surveying sites

Kyoichi KOYAMA	(Metal Mining Agency of Japan)
Katsutoki MATSUMOTO	(Metal Mining Agency of Japan)
Seiichi ISHIDA	(Metal Mining Agency of Japan)
Yoshihisa YAMAMOTO	(Metal Mining Agency of Japan)
Seizo NAKAO	(Geological Survey of Japan)

Members of the surveying team

Chief

Toshio TAKAHASHI	(Deep Ocean Resources Development Co.: DORD)
------------------	---

Members

Chief geologist Kazuo SANO	(DORD)
Geologist Kiyoshi TONO	(DORD)
" Yutaka YOSHINAGA	(DORD)
" Yoshikazu YOKOYA	(DORD)
" Masahiro NISHIGUCHI	(DORD)
" Yasunori EGAWA	(DORD)
" Toru OI	(Ocean Engineering and Development Co., Ltd.)
Geologist Yutaka HASHIMOTO	(Ocean Engineering and Development Co., Ltd.)
Chief Geophysicist Kenji KONAGAI	(DORD)
Geophysicist Hiroshi MATSUYAMA	(DORD)
" Shiro OYAMA	(DORD)
" Hiroo SAITO	(DORD)
" Kazunori MATSUI	(DORD)
" Nobuyuki MURAYAMA	(DORD)
" Terumi YAMAMICHI	(DORD)
" Yoshiki IMAI	(DORD)
" Yutaka WATANABE	(Ocean Engineering and Development Co.,Ltd.)

Consigning side

Negotiators for the agreement

Jioji KOTOBALAVU (CCOP/SOPAC)

C.A.MATOS (CCOP/SOPAC)

C.L.TIFFIN (CCOP/SOPAC)

Advisor

D.S.CRONAN (CCOP/SOPAC)

1-6 Apparatus and Equipment for the Survey

The major apparatus and equipment used during the survey are shown in Table 1-1.

Table 1-1 Apparatus and Equipment for the Survey

	Survey Method	Survey Apparatus and System	Abbreviation	Remarks
Positioning	Satellite navigation	Navy navigation satellite system	NNSS	
		Global positioning system	GPS	
Sea bottom topography and Geological survey	Acoustic sounding Bathymetry Topography	Precision depth recorder	PDR	
		Narrow beam echo sounder	NBS	
	Sea bottom surface	Multi-frequency exploration system	MFES	
	Subsurface geologic structure	Sea-bottom profiler	SBP	
	Sampling Grab with finder	Free fall grab Spade corer Arm-type dredger Chain bucket	FG SC AD CB FPG	Towing type
Sea bottom obstruction		Free fall camera Continuous deep-sea camera with finder	FC FDC	Towing type
Data recording and processing	On-line data, track line maps, bathymetric maps, various plan maps, cross sections, sampling maps etc.	S 20 Data processing unit Data control room system if 800 personal computer	CPU DCS	

1-7 Records of the Survey

The survey operations were accomplished as shown in Table 1-2 and Table 1-3.

Table 1-2 List of Survey Achievements (1)

	Item	Accomplishment
Survey Schedule	Leaving Majuro	Aug., 28 16:00 (in local time)
	Arriving in the survey area	Aug., 31 05:30
	Leaving the survey area	Sep., 17 17:00
	Arriving at Suva	Sep., 19 08:30
	Leaving Suva	Sep., 22 16:00
	Arriving in the survey area	Sep., 24 05:00
	Leaving the survey area	Oct., 19 00:00
	Arriving at Honolulu	Oct., 25 08:00
Sampling	(Manganese Nodules) Sampling interval Sampling stations Sampling per station Total sampling Samplers used Failure due to non-floating	Primary: 00 mile grid Primary: 24 points, 3 samples 72 points (24x3) Free fall grab (FG): 68 samplings Spade cores (SC): 4 samplings None
	(Cobalt Rich Crust) Number of seamounts Sampling stations Samplers used Amount of samples recovered	8 seamounts 89 points arm-type dredge (AD): 62 points chain bucket (CB): 25 points grab with finder (FPG): 2 points 2,695 kg (including substrates)
Deep-sea camera	(Manganese nodules) Use of camera Acquired photographs	Deep-sea camera 72 times 61
	(Cobalt crusts) Acquired photographs	FDC 756 (5 seamounts, 6 track lines, 37.2 miles)
	Acquired VTR tapes	17

Table 1-2 List of Survey Achievements (2)

	Item	Accomplishment
Analysis	Number of analysis Analyzed components Total number of analyzed components	Manganese Nodules: 87 cases Cobalt Crusts: 169 cases 5 components (Ni, Cu, Co, Mn, Fe) 1,280 (256 x 5 components)
Acoustic sounding	(Manganese Nodules) NBS (30.0 kHz) PDR (12.0 kHz) SBP (3.5 kHz) MFES	Length of traverse 3,278 miles " " " " " "
	(Cobalt Crusts) NBS (30.0 kHz) PDR (12.0 kHz) SBP (3.5 kHz)	Defective traverse 0 mile " " " "
Data processing	On line MT MIX MT Sampling MT MIX MT Weather-Sea state MT MIX MT	10 reels 10 " 1 " 1 " 1 " 1 "

Table 1-2 List of Survey Achievements (3)

	Item	Accomplishment						Total (av)
	Track line	88SFDC01	88SFDC02	88SFDC03	88SFDC04	88SFDC05	88SFDC06	
FDC	Date	09/06	09/25	09/25	09/29	10/06	10/13	-
	Seamount	SB01	SB02	SB02	SB03	SB06	SB08	-
	Track line length (A) (miles)	5.6	5.6	0.6	7.9	10.2	7.3	37.2
	Survey duration (hrs)	06:29	07:00	00:45	06:12	08:54	06:51	36:11
	Equip. throw-in time	07:01	07:23	15:31	06:33	09:12	11:52	-
	Time spent on photography (T) (hrs)	04:44	05:45	00:35	04:53	07:19	05:17	28:33
	Equip haul-in time	13:30	14:23	16:16	12:45	18:06	18:43	-
	Av. speed (A/T) (kts)	1.18	0.97	1.03	1.62	1.39	1.38	1.30
	Av. time for each photo (min.)	1.79	3.00	1.13	2.40	2.30	2.30	2.27
	Number of photos	159	115	31	122	191	138	756
	Number of records (reels)	3	3	1	2	4	2	15

	Item	Accomplishment		
	Track line	88SFPG01	88SFPG02	Total
FPG	Date	10/01	10/09	-
	Seamount	SB03	SB06	-
	Track line length (A) (miles)	0.11	1.45	1.56
	Survey duration (hrs)	01:49	02:48	04:37
	Equip throw-in time	12:28	11:34	-
	Observing time (T)	00:36	01:25	02:01
	Equip. haul-in time	14:17	14:22	-
	Av. speed (A/T) (kts)	0.18	1.02	0.77
	Collected sample (kg)	0.303	225.0	225.303
	Records (reels)	1	1	2

Table 1-3 Records of Survey Schedule

Duration: 62 days, Survey, duration: 43 days

Month/day		Survey Items	Month/day		Survey Items
8/26	Fri	Pre-TV filming meeting	9/26	Mon	Co crust survey (SB02)
27	Sat	TV filming	27	Tue	" "
28	Sun	Lv. Majuro (16:00)	28	Wed	" (SB03)
29	Mon	Training planning	29	Thu	" "
30	Tue	Preparations	30	Fri	" "
31	Wed	Mn nodule survey	10/1	Sat	" "
9/1	Thu	"	2	Sun	" (SB04)
2	Fri	"	3	Mon	" "
3	Sat	"	4	Tue	" "
4	Sun	Co crust survey (SB01)	5	Wed	" (SB05)
5	Mon	" "	6	Thu	" (SB06)
6	Tue	" "	7	Fri	" "
7	Wed	" "	8	Sat	" "
8	Thu	" "	9	Sun	" "
9	Fri	Mn nodule survey	10	Mon	" (SB07)
10	Sat	"	11	Tue	" "
11	Sun	"	12	Wed	" "
12	Mon	"	13	Thu	" (SB08)
13	Tue	"	14	Fri	" "
14	Wed	"	15	Sat	" "
15	Thu	"	16	Sun	" "
16	Fri	Seamount topography preliminary survey	17	Mon	Mn nodule survey
17	Sat	"	18	Tue	"
18	Sun	Travel	19	Wed	Surv. completed (00:00)
19	Mon	Ar. Suva (08:30)	20	Thu	Travel
20	Tue	SOPAC meeting, ship open house	21	Fri	"
21	Wed	Off	22	Sat	"
22	Thu	SOPA meeting, Iv. Suva	23	Sun	"
23	Fri	Preparations	24	Mon	"
24	Sat	Ar. survey area topographic survey	25	Tue	Ar. Honolulu (08:00)
25	Sun	Co crust survey (SB02)	26	Wed	Transfer to succeeding team

Note: Mn-nod. survey 13 days
 Co crust survey 30 days
 (SB01)~(SB08): seamounts

Chapter 2. Survey Methods

2-1 Manganese Nodules

1) Survey Procedures

Zones with water depth suitable for manganese nodule occurrence were selected from the survey area and 24 stations were set. Free fall sampling at these stations and various acoustic sounding were carried out during the primary (reconnaissance) survey. It was planned that we would proceed to the next survey if favourable results were obtained by the primary survey. The results, however, were disappointing and we were obliged to cancel the detailed work.

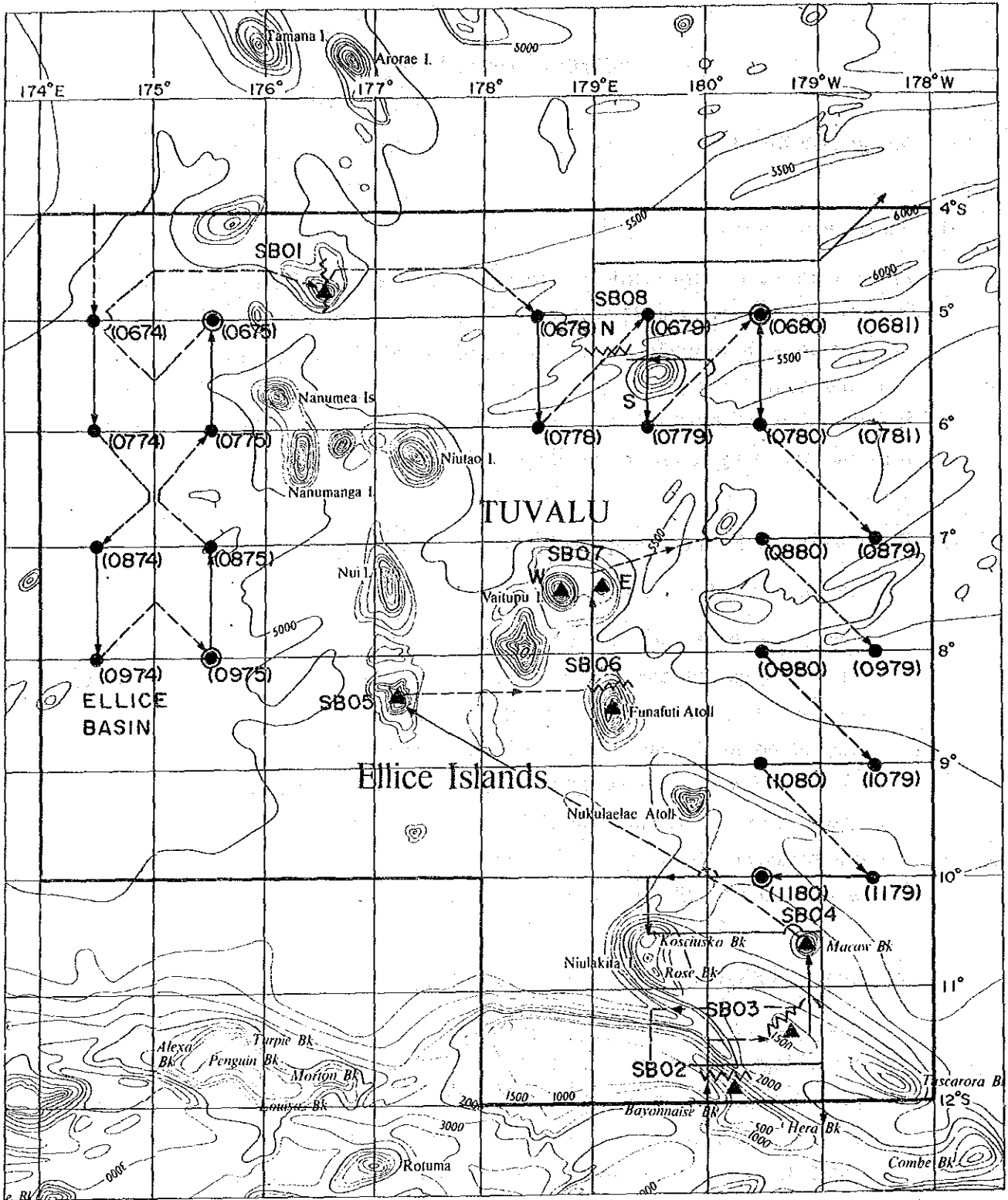
2) Numbering Track Lines, Sampling Stations and Sampling Points

(1) Numbering of the track lines

The track lines for acoustic sounding (PDR, SBP, NBS, and MFES) were numbered, so that the date and the order of work could be identified by every cruising unit; for instance, 88S0925A, 88S0925B. For the night cruising "N" was added to the end of numbers such as 88S0925N. For the lines merely between sampling points, "P" (Passing) was added such as 88S0925P. In these cases, "88S" means the financial year of the survey (1988) and the executing organization (SOPAC); "0925" indicates the month of September and the date of 25th, and "A, B" the order of track lines on that day.

(2) Numbering sampling stations and sampling points

"88S" was prefixed to indicate the financial year of the survey (1988) and the executing organization (SOPAC). The survey area was divided into quadrilaterals by longitudinal and latitudinal lines at every 1°. To those quadrilaterals, four-digit area-code numbers were designated as shown in Fig. 2-1. In those numbers, the first two figures designate the south side latitudes and the last two figures indicate the last two digits of the west side longitudes of the quadrilaterals. However, these squares contain north and west sides of the numbered area and not east and south sides. The sampling carried out in the areas were numbered with additional figures beginning from "01", indicating the respective sampling methods.



LEGEND

- Survey area
- Sampling station for manganese nodule
- ▲ SB01~SB08 Seamounts for cobalt crust survey
- ⊙ Sampling site by spade corer
- Daytime navigation
- - - Nighttime navigation
- (0674) Areal block number
- ⚡ FDC survey line

Figure 2-1 Location Map of Survey Stations, Seamounts and Others

Example: The sample number "88S0674FG01" indicate collected by FG (Free Fall Grab) in the area 0674 SOPAC in 1988.

3) Ship Positioning

During the survey, all the ship positions were indicated by "NNSS" and "GPS". In the case of NNSS, "Corrected positions" were used (Annexed Fig. 1). These were calculated by using the time difference between the satellite determined "up-date" positions and proportionately determining the ship's position. The ship positions were registered in the field note for subsequent use in data processing and anylysis. The items recorded are as follows.

- i) Starting and terminating positions on the track lines, course changes, positions at every on the hour.
- ii) Samplers setting positions and their re-collecting positions.

All the ship positions relating to the survey activities were registered in on-line MT by using the data processing system on board. Also, the corrected vessel positions were printed out by the same system every minute for use in compiling and analyzing the survey data.

4) Sea Floor Topography

Sea floor topography, observation and depth measurement were done mainly by NBS between the stations and between sampling points. Moreover, in the case of FDC, the sea-floor topography studies in the vicinity of the track lines were made before the camera observation. The sounding was carried out every 12 seconds and the values indicated by NBS digitizer were registered in on-line MT. In addition, every 5 minutes, water depth was recorded on NBS, and the sea floor topographic map was drawn with these data. The survey between stations was generally done at 10 knots, but with varying conditions, the speed was accordingly changed. As for the track lines between the sampling points, the speed varied in the range of 3-8 knots according to the sampling operation.

5) Surficial Sediments

The survey of the surficial sediments was carried out by 3.5 kHz SBP on all track lines simultaneously with the sea floor topography survey. The basic information regarding surficial sediments consists of data on the thickness of the uppermost transparent layers of the SBP records, seismic stratigraphic type and other data.

These data were also recorded in the field book every 5 minutes and used for preparing surficial sediments isopach map and SBP type distribution map.

6) Manganese Nodule Survey by MFES

The survey of the abundance of manganese nodules was made by MFES simultaneously with the survey of the sea floor topography and the surficial sediments. The MFES data were calculated from NBS, PDR and SBP data every 48 seconds, however, moving average of 15 measurements was used as MFES values. The MFES data were recorded in MT by data processing system and in the MFES floppy-discs every 5 minutes.

7) Sampling and Sea Bottom Observation by Deep-sea Camera

Sampling was carried out mainly by FG (Free Fall Grab) and partially by SC (Spade Corer). In addition to the sampling, the sea floor was photographed by deep sea camera mounted on the samplers. The sampling density of the primary survey was 60 mile grid. Sampling sites are shown in Annexed Fig. 2.

At every station, three samplings were done in the following manner. The station was set at the southern apex of a right-angled isosceles triangle with 1.4 miles as the length of the equal sides. Sampling was done at the three apexes of the triangle namely at a distance of 1.4 miles to the northeast and northwest of the station as shown in Figure 2-2.

When using SC rather than FG, the first sampling, as a rule, was done by SC. In rare cases, with FG, in sufficient sampling due to net damage or incomplete operation is inferred. In such cases, the grab operating accuracy is calculated by comparing the coverage of the manganese nodules by sea bottom photography with the samples collected. The grab accuracy is used as reference in calculating the abundance.

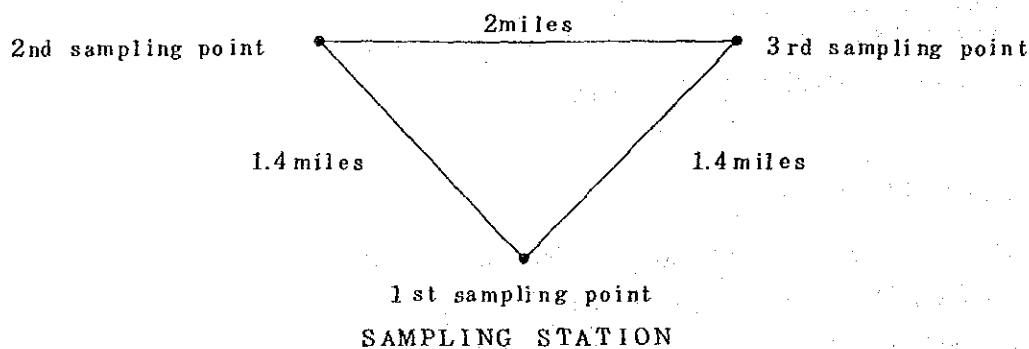
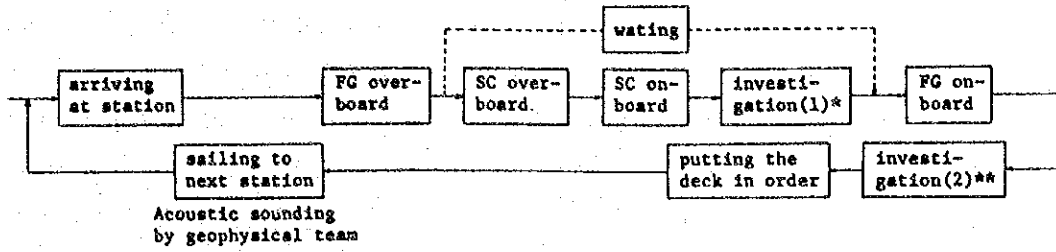


Figure 2-2 Explanation on Setting Order of Three Samplers at a Sampling Station

[A] The outline of the bottom sampling work



* Detail of investigation (1)

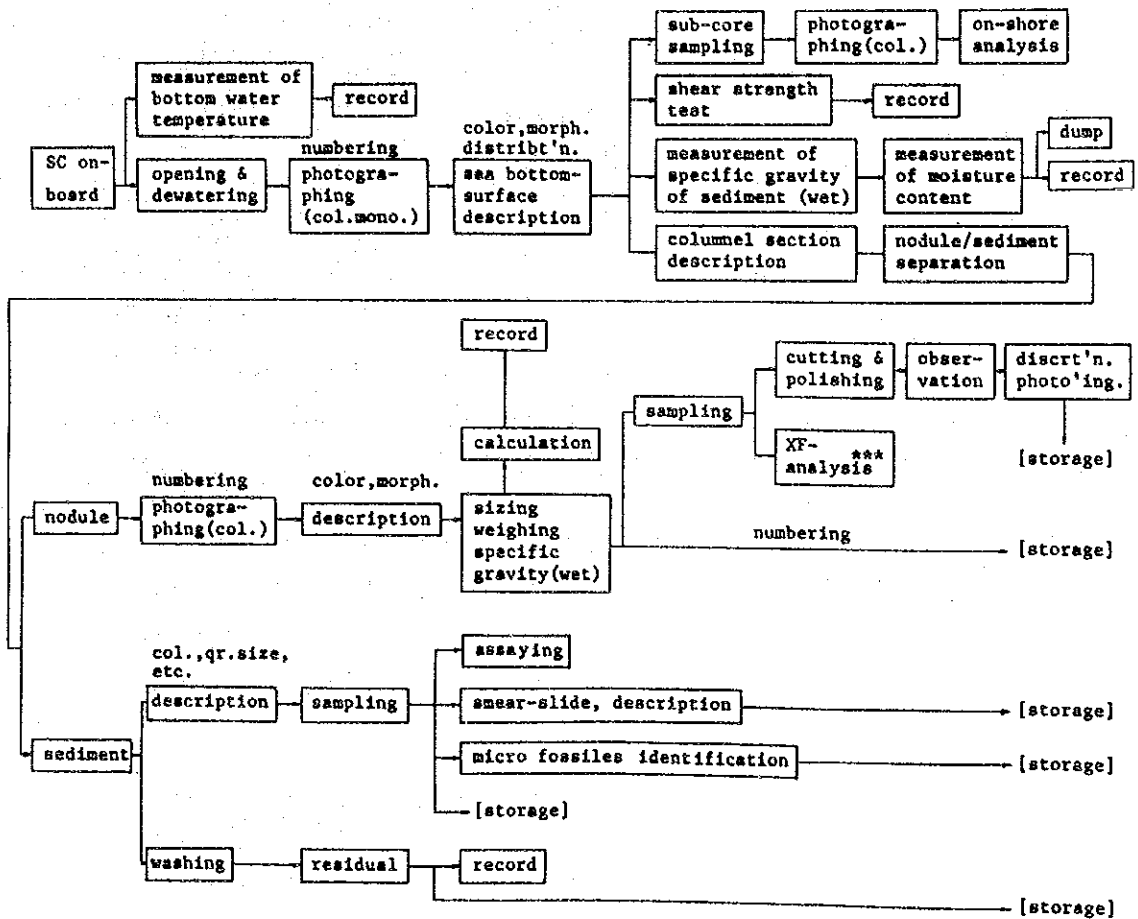
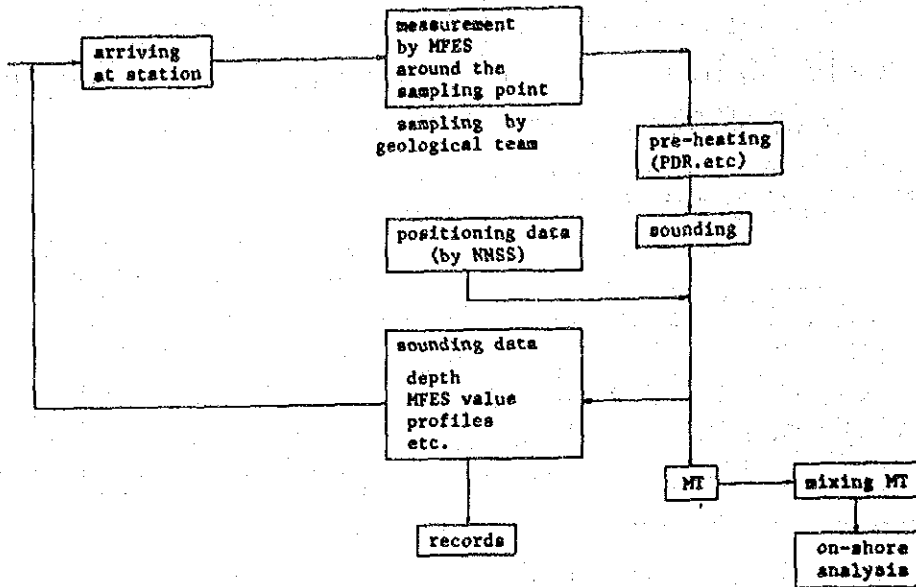


Figure 2-3 Processing and Assaying Flowsheet of Samples (1)

[B] The outline of the acoustic sounding



After surveying, on the way to the base harbor, all data are analyzed and evaluated. The outline of them are as follows:-

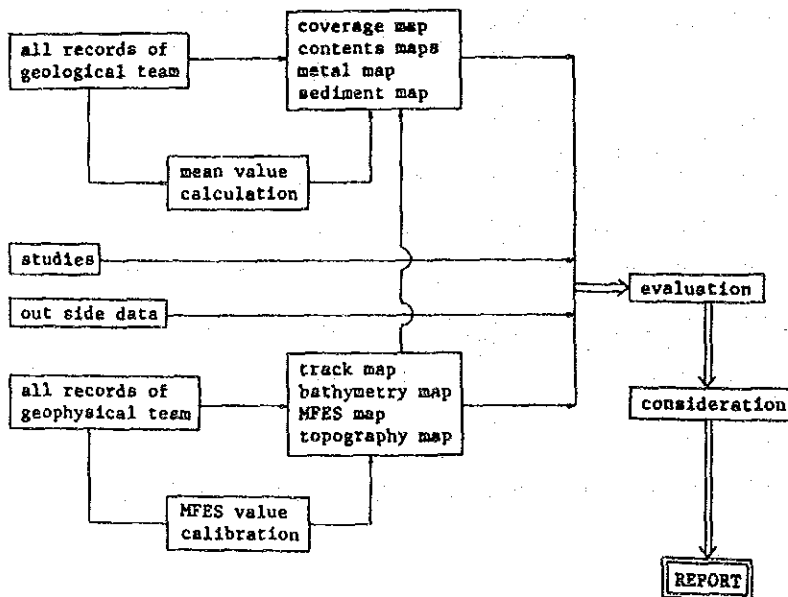


Figure 2-3 Processing and Assaying Flowsheet of Samples (2)

8) Processing, Analysis and Storage of Samples

The collected samples (manganese nodules and bottom materials) were processed on board, mainly following the processing and analyzing flowsheet of FG·SC samples including various measurements and X-ray fluorescence as shown in the Fig. 2-3 (1), (2), some of them were also selected for further microscopic observation, X-ray diffraction, complete analysis, minor-element analysis, and other work at the laboratory and the rest were kept in storage.

9) Processing and Analysis of the Survey Data

The processing and analysis of the survey data were carried out mainly on board, however, a part of the data processing, analysis and interpretation was done on shore.

(1) Survey data and processing

- The ship positions by NNSS (date, time, latitude, longitude) were printed out in the table of corrected positions every minute from the data processing system on board.
- The depth data by NBS (date, time, values reported from the digitizer and in the print-out papers) were registered in the field book every 5 minutes.
- The surficial sediments by SBP (thickness of the uppermost transparent layers, stratigraphy type) were registered in the field book every 5 minutes.
- The values measured by MFES were registered in the field book every 5 minutes on the track lines between the sampling points and on the track lines between the observation points. The following survey data on manganese nodules, sediments, assay and others were registered in the field book for every sampling point.
- Data regarding manganese nodules; sampled amount, wet weight, wet specific gravity, morphology, number, surface structure, etc. for each class of sized manganese nodules.
- Data regarding sediments; type of sediments, colour tone, grain size, microfossils, etc.
- Data regarding assay; grade of 5 principal components (Ni, Cu, Co, Mg, Fe) and water content.

- Sea bottom photos by deep-sea camera mounted on FC and SC, hauling-in photos, working photos.
- Record photos of geophysical survey (NBS records, SBP records)

(2) Analysis of the survey data

The essential maps and tables were drawn on board using the data available. These data were later analyzed in further detail on shore. The results of the analysis are shown in the following maps and tables (Fig. 2-4).

i) Maps of track lines, location maps of sampling points

The maps of track lines and the location maps of sampling points were prepared by plotting the position on a 1/1,200,000 scale registering sheet based on the table of corrected positions printed out from the data processing system.

ii) Sea-floor topographic maps

Using the bathymetric charts obtained by plotting depth values every 5 minutes on the above-mentioned track lines charts, the sea-floor topographic maps were drawn with contour intervals of 200 m.

iii) Isopach maps of the uppermost transparent layers by SBP

The thickness of the uppermost transparent layers was read out every 5 minutes from the SBP record and plotted on the above track line charts. Then the isopach maps were completed with contour intervals of 10 m.

iv) Distribution maps of sediments

Distribution maps of sediments were prepared by plotting the sediments collected by the sampler and the quantity of authigenic minerals.

v) Abundance of manganese nodules estimated by MFES

Abundance maps of manganese nodules were prepared by plotting the MFES data displayed every 5 minutes. Abundance contour lines was drawn with interval of 2.5 kg/m².

vi) Abundance maps of manganese nodules, grade contour maps, metal content maps

On the basis of data obtained on the manganese nodules at each sampling point (FG, SC lowering point), the average state of ores (abundance,

grade etc.) were obtained for each station (3 samplings per station). On the basis of these results, the abundance maps of manganese nodules, the grade contour maps of nickel, copper, cobalt, manganese and iron and the metal content maps of nickel, copper, and cobalt were prepared. The acoustic sounding data were also utilized in this process.

vii) Table of the survey results

In order to facilitate the searching and consulting of the data on the manganese nodules obtained on board every day, the essential items*1 were excerpted from the field book and annexed in table form.

*1 The principal items; latitude, longitude, water depth, grain size distribution, abundance, morphology, grade, sediments, states of combination, etc..

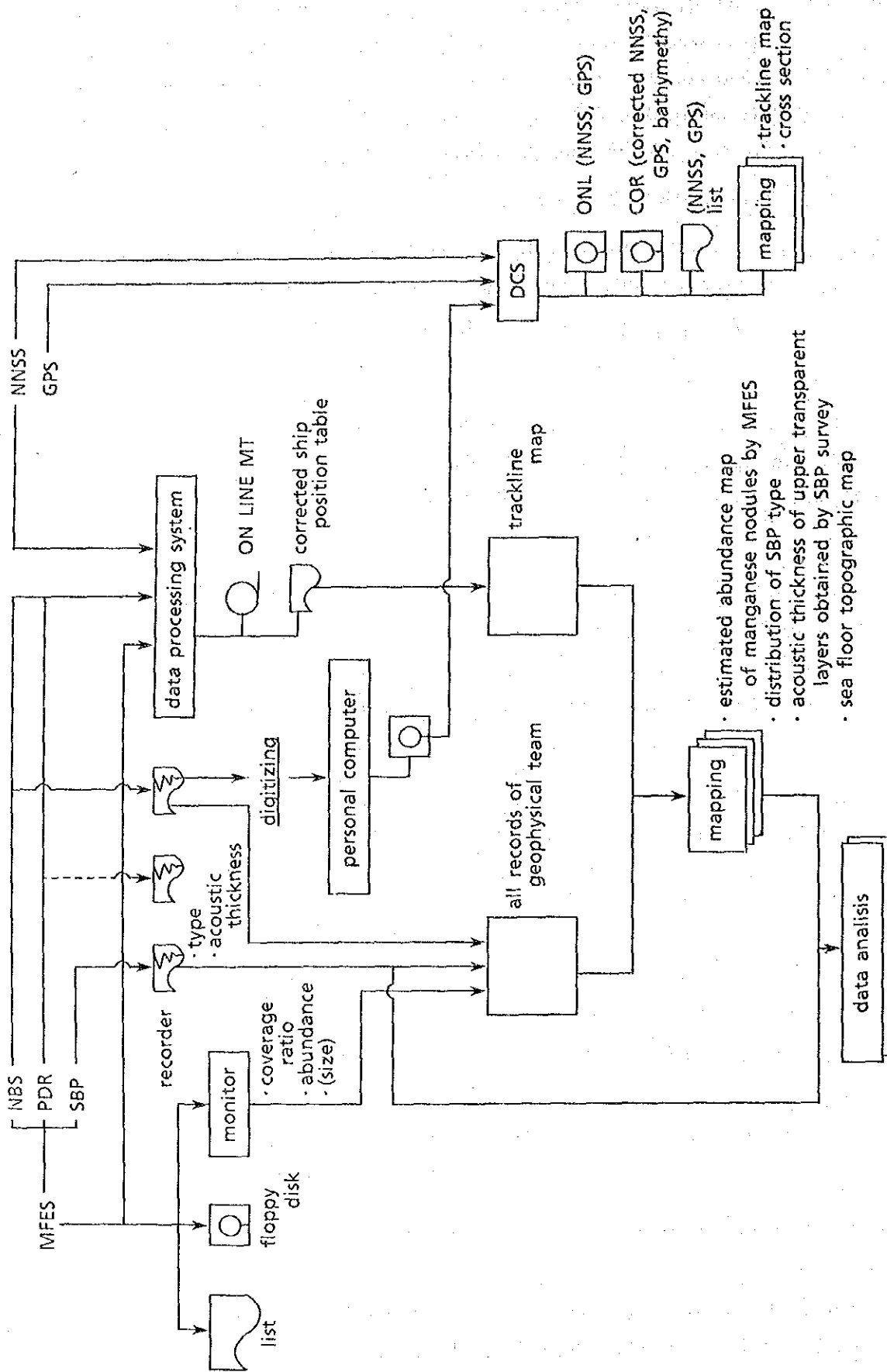


Figure 2-4 Acoustic Sounding and Processing Flowsheet (Manganese Module)

2-2 Cobalt Crusts

1) Survey Procedures

Eight seamounts were selected on board for survey, based on both previously known and newly obtained from sea-floor topographical data (Fig. 2-1). These eight seamounts include two atolls (Funafuti, Vaitupu Is). The survey mainly consisted of investigating the seamount topography and surficial sediments by acoustic sounding and of sampling by dredges. Partially, the sea bottom observation and photography by FDC were carried out.

2) Numbering Track Lines, Sampling Stations and Sampling Points

Numbering the seamounts was done as follows.

(Seamounts) S (SOPAC) TUVALU (B...begin with B, apply C,D...successively for other sea areas from the next year) - Number.

Example: SB01.

(Sampling points)

Year-seamounts-type of dredge-No.

Example: 88SB01AD01

(FDC track lines)

Year-S(SOPAC)-FDC-No.

Example: 88SFDC01

(Track lines for acoustic sounding)

Year-S(SOPAC)-data-N(night)

Example: 88SO901N

(Apparatus and equipment used in the survey)

These are shown in Table 1-1

3) Ship Positioning

The ship positioning used was the same as that for manganese nodule survey.

4) Sea-Floor Topography

The sea floor topography was obtained by NBS and PDR etc. The sea floor topographic maps were drawn with a plotter. The designed standard distance between the track lines was 4 miles and 2 miles if necessary. The ship speed was normally 10 knots.

5) Surficial Sediments

The distribution of surficial sediments of the seamounts was obtained by means of SBP. The data was used for selecting the sampling points.

6) Sampling

Sampling was carried out by dredges on all eight seamounts. Many types of dredges were used for various purposes (Table 1-1). The target areas were the top and slope of the seamounts down to the depth of 3,500 m. Sampling was done at about ten points on each seamount. The ship speed was 0.5~1.5 knots during dredging. The standard towing time between the dredges on and off bottom was approximately 30 minutes.

7) Processing, Analysis and Storage of Samples

The dredged samples were weighed and described after being classified into several types on board. A part of every sample was analyzed for five components; Co, Ni, Cu, Mn, Fe, and water content. The method of analysis was the same as for manganese nodules, however, the tests for deviation of data (the bias tests) were made on the same samples on shore. Microscopic observation, X-ray diffraction, total analysis, micro-analysis, etc., were carried out on shore as in the case of manganese nodules. Some typical samples were stored water-sealed in plastic bottles, and the rest were stored dry in wooden boxes.

8) Sea Bottom Observation by FDC

In order to observe the mode of occurrence of cobalt crusts and to photograph typical occurrences. FDC was used on five seamounts. The designed length of tracks was 5 to 10 miles, and the standard speed was 1.0 knot during the observation. In principle, the photos were taken continuously along the sea bottom. Interval time between the shots were not fixed. A TV camera with finder was loaded on the FDC vehicle, so that the real time observation and detailed observation was possible by VTR. The mode of occurrence of cobalt crusts,

especially the coverage and the lateral variation of crusts which could not be obtained from the sampling, could be analyzed by the VTR and photographs.

9) Processing and Analysis of the Survey Data

(1) Survey data and processing

These were basically the same as in the case of manganese nodules. However, MFES was not used in the cobalt crust survey. And FDC was used instead of FG, SC and other methods. Operational flow is shown in Fig. 2-5.

(2) Analysis of the survey data

The results of the on board and on shore analysis are shown in the following charts and tables.

i) Maps of track lines

A Map of track lines was drawn at the scale of 1/300,000 for each seamount.

ii) Maps of sea-floor topography, location maps of sampling points

Maps of sea-floor topography was prepared at 1/300,000 scale by X-Y plotter and the approximate sampling points were plotted.

iii) Cross sections of sea-floor topography

Based on the data of (ii), the cross sections of sea-floor topography was drawn by X-Y plotter.

iv) Geological maps of sea-floor and abundance maps of cobalt crusts

A map was completed for every seamount showing the dredge sampling data and FDC data on the sea-floor topographic map. The average grade of each sampling was also shown in the map.

v) FDC observation survey maps

The mode of occurrence of cobalt crusts obtained from VTR and photo analysis, FDC track lines of sea floor topographic, cross section the estimated cobalt crusts coverage, were shown as route maps.

vi) Various maps showing relevant features were prepared in order to study the resource potential of cobalt crusts.

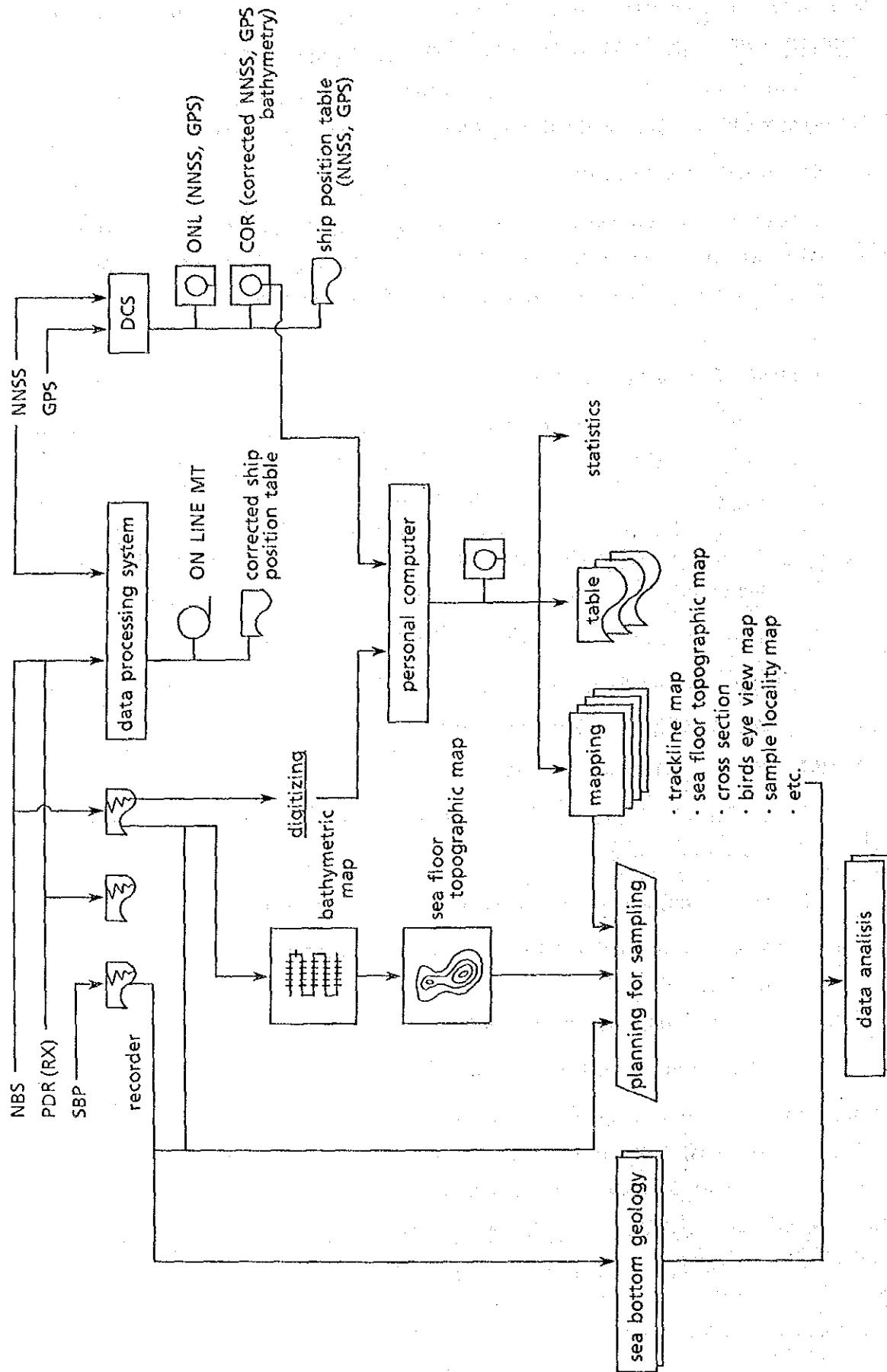


Figure 2-5 Acoustic Sounding and Processing Flowsheet (Cobalt Crust)

Chapter 3. Results of the Survey (Manganese Nodules)

3-1 Sea-Floor Topography

1) Regional Topography

The sea-floor topography of the whole survey area are shown in Fig. 3-1-1 and Annexed Fig. 3. Ellice Island chain is developed in the central part of the survey area and divides the area into western Ellice Basin and the eastern North Tokelau Basin. The western part of the survey area belongs to the eastern margin of the Ellice Basin and the water depth range is 5,000~5,400 m (average 5,300 m) with the exception of the seamounts and hills. The eastern part of the survey area consists of the western margin of the Nova-Canton Trough, Central Pacific Basin and the North Tokelau Basin and the relief is generally larger than the western part. The water depth of this part ranges from 5,200 m to over 6,000 m gradually increasing northward.

Seamounts exceeding 3,500 m in relative height were confirmed at two localities (Seamount SB08(N)-(S): summit depth 1,450 m, 1,230 m and a seamount newly discovered by this survey with summit depth 1,890 m). These seamounts intersect the western margin of the Nova-Canton Trough obliquely and are arranged in northwest direction nearly parallel to the seamount chain of the mountainous province. In this province, islands of the Tuvalu-Ellice Islands, Funafuti and nine atoll islands and various seamounts and knolls extend in northwest direction. These are in the central part of the survey area.

The seamounts are classified into atolls (SB06; Funafuti Is., SB07(W), Vaitupu Is), flat summit seamounts (SB01, SB02, SB03, SB04, Macaw Bank, SB08), peaked seamounts (SB05, SB07(E), SB08(N)) and others. The morphology of these seamounts will be mentioned in detail in the section on crust survey.

2) Classification of Sea-Floor Topography

In order to clarify the mode of manganese nodule occurrences, the floor topography was classified from both macro- and micro-topographic point of view. Definitions of topographical classification are shown in Table 3-1-1. The sea-floor topography of the present survey area can be largely divided into three provinces, namely the plain in the west (west of 176°E), mountains in the centre and the quasi plain in the east (east of the line 4°S, 176°30'E - 9°30'S, 178°W).

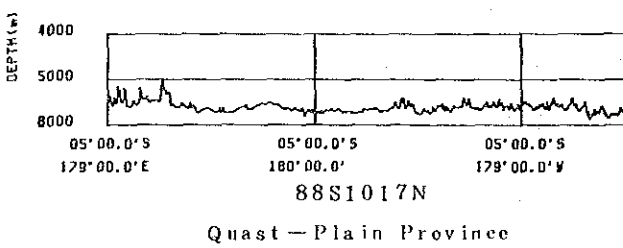
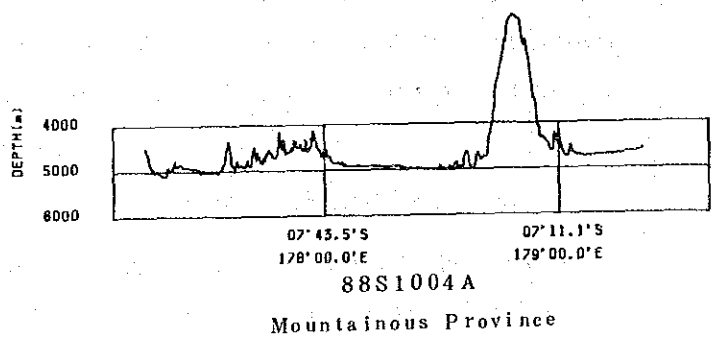
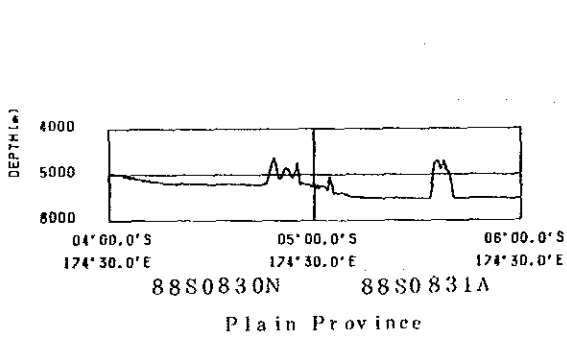
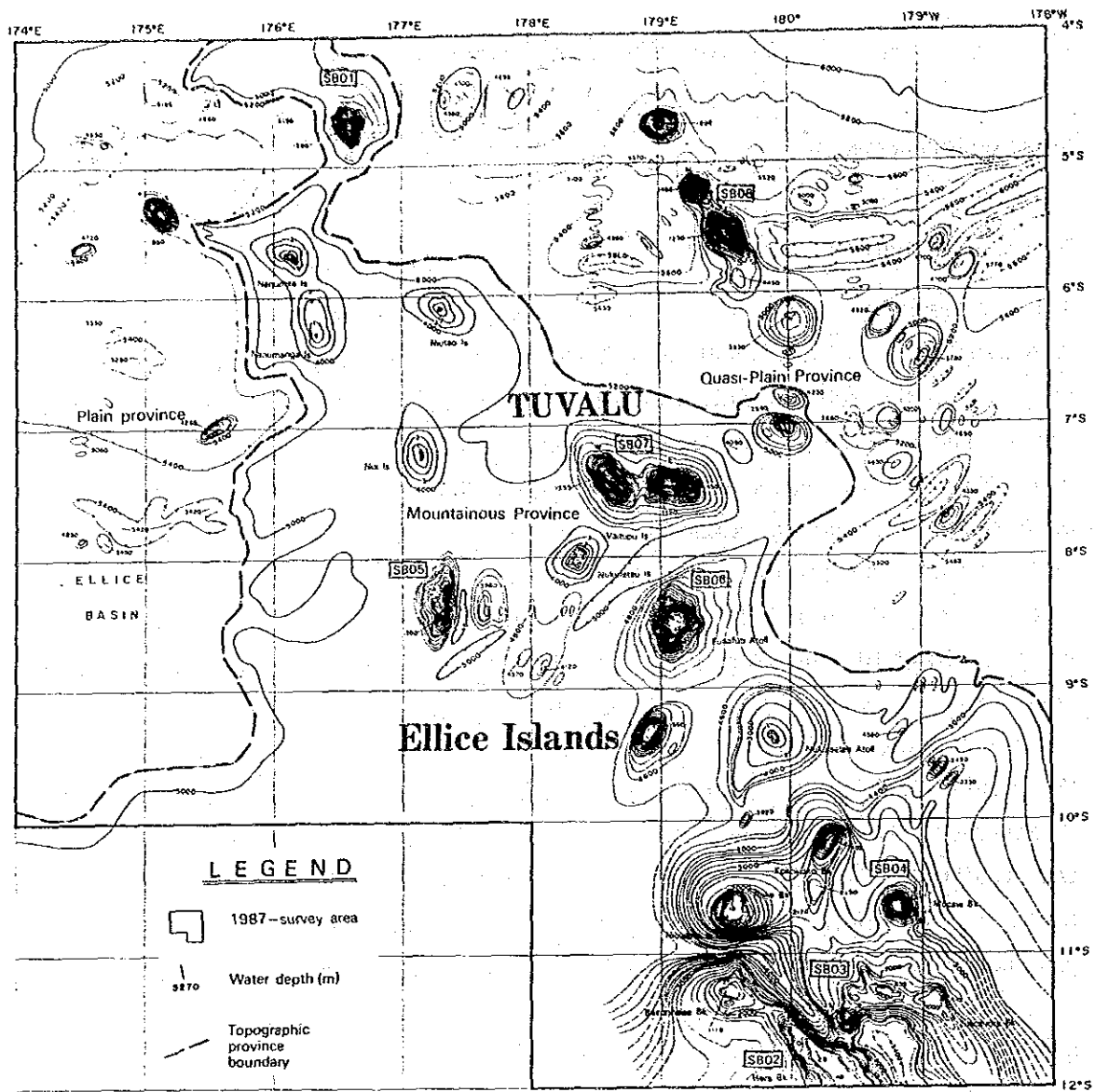


Figure 3-1-1 General Sea Floor Topography (Plan)

These macro-topographic features correspond to the following areas.

- i) Plain; eastern margin of Ellice Basin.
- ii) Mountains; a part of Ellice islands.
- iii) Quasi plain; the western margin of North Tokelau Basin.

Table 3-1-1 Classification of Sea Floor Topography

Topographical classification		Definition
Regional province	Plain	Area where the sea-floor is almost flat and with isolated seamount or sea knolls, it may be considered as plain from a general point of view.
	Hill	Area where numerous sea knolls or seamounts are dispersed.
	Mountainous	Area where the outstanding mounts or knolls are rarely observed but the bottom is rather undulated and which can classified neither as plain nor as hilly.
	Quasi-plain	
Local area	Flat	Plain area not undulated or smoothly undulated (up to about 100 m relative height) and which does not belong to the hollow or the platform.
	Hollow	Area with smooth undulation and which presents a generally concave terrain, including a ship-shaped basin.
	Channel	Long and narrow concave terrain in a ditch shape, including fissures or fracture zones.
	Platform	Area with smooth undulation which presents as a whole a convex terrain (or a tableland).
	Sea knoll	Hilly area with a relative height of less than about 1,000 m, including entire slope as well as summit.
	Seamount	Hilly area with a relative height of more than about 1,000 m, including entire slope as well as summit (the sloping surface contains a shifting part of the plain),
	Ridge	Terrain presenting a chain of mountains composed of the sea knolls and hills ranged in a zone.
Other	Terrain not belonging to any of the above-mentioned classifications.	

The micro-topography of the survey area is classified into the seven categories listed in Table 3-1-1. They are:

Flats; widely distributed in plains and the along the border of the quasi plains and themountainous areas.

Hollows (including ship-shaped basins);

small scale hollows occur scattered in western plain and quasi plains.

- Channels; occur in the southern side of the mountainous province.
- Platforms; occur scattered in the plain as minor constituent.
- Sea knolls; occur scattered in the plain and quasi plain and are aligned parallel to the seamounds of the mountainous province.
- Seamounts; occur throughout the mountainous province aligned in northwest direction. To the south of the seamounds, groups of banks occur with shallow summit depths of several tens of meters.

As above, in the western plain, there are only a few scattered knolls and platforms, thus the morphology is not clearly known. The eastern quasi plain has greater relief compared to the western part.

Topography with mountains and valleys repeating with short wavelength was confirmed in a part of the northern side of the quasi plain.

3-2 Surficial Sediments

1) Classification of SBP Records (Fig. 3-2-1)

SBP records are classified into six types: type b, type c, type d₁, type d₂, type d_s and type e₁ based on their reflection patterns in the survey area. Definitions and characteristics of each type are as follows:

i) Type in which the acoustic transparent layers are recognized in upper layers.

Type b; composed of two layers, transparent and opaque, but the transparency of transparent layer is not high and is translucent. Thickness is 10~60 m.

Type e₁; has multistratified structure of transparent and opaque layers, particularly the transparent layers of the western part almost always show four reflections with equal distance among the top three. Many of the lower opaque layers are multistratified.

ii) Type for which the acoustic transparent layers are not recognized in the upper layers.

Type c; shows three layered structure, transparent-opaque-transparent. Also in some areas, alternations of thin transparent and opaque layers are classified in this category. The opaque layer is inferred to be sediments and igneous rocks with high reflectivity (the fine alternation of transparent and opaque in the western plain, however, is turbidite). When low reflectivity material such as clay are collected from type c area, it is probably due to the fact that the transparent layers are thinner than the resolution of SBP and could not be detected.

Type d₁; composed only of opaque layers. Generally, this type is found at seamounts, knolls, etc., and most of these sites correspond to the exposed basement rocks.

Type d₂; composed only of opaque layer, and this type is observed mainly in plains and these sites correspond to basement rocks or coarser grained sediments. A part of those found in the western plain is considered to be turbidite deposits.

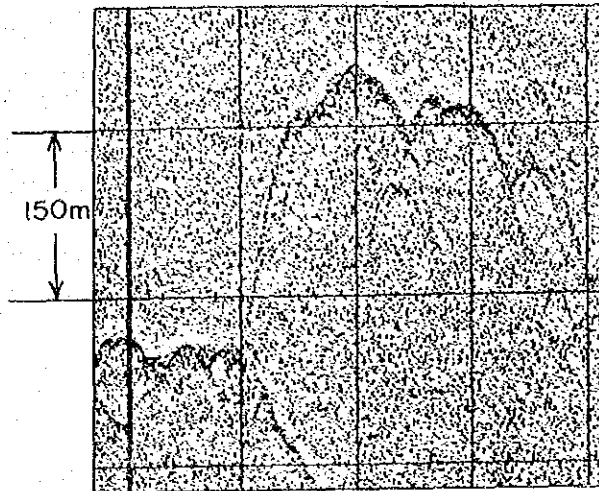
Type d₂

Line No. 88S0914A
9°00'S · 179°15'W



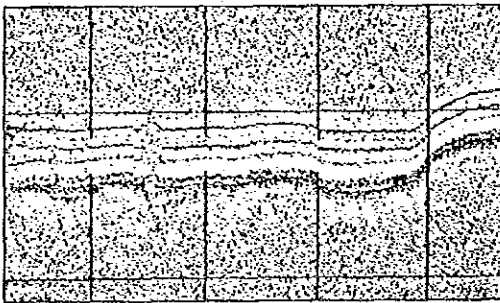
Type d₁

Line No. 88S0903A
5°36'S · 175°30'E



Type e₁

Line No. 88S0901N
7°43'S · 174°49'E



Type b

Line No. 88S0903N
4°42'S · 174°49'E



Type c

Line No. 88S0831A
5°45'S · 174°30'E



Type ds

Line No. 88S0902N
6°36'S · 175°06'E

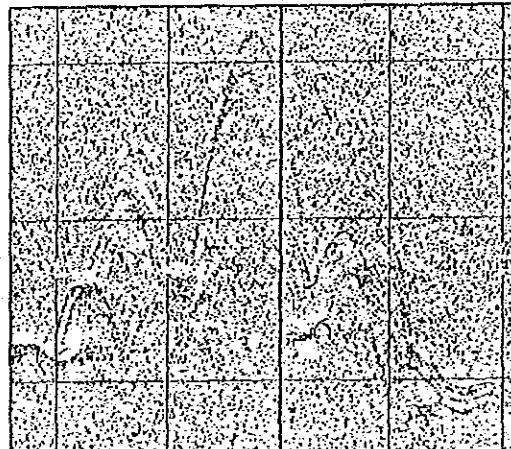


Figure 3-2-1 Classification of SBP Records

iii) Other types

Type ds; considered to be composed only of opaque layers, the records are not clear because of the dispersion of sound waves by the undulating floor. This type is observed mainly in the hilly parts of the survey area.

2) Distribution of SBP Types (Annexed Fig. 4)

The distribution of SBP types and transparent layers in i) plain, ii) mountainous and iii) quasi plain provinces is as follows. The SBP track line interval of this survey area is wide, thus the SBP results are linear data and the accuracy of planar distribution is not high.

i) Plains (western part of the survey area)

The SBP records of this area are of types c, d₁, d₂ and e₁. The area north of 6°30'S contain mostly types c and d₂ without the upper transparent layer, d₂ occurs particularly north of 5°S. In the area south of 6°30'S, type e₁ the with upper transparent layer, is the major record obtained the concentration of type d₁ is mainly observed near 6°30'S, 175°E and 5°S, 175°30'E. The distribution of ds is sporadic probably due to the flat sea-floor.

ii) Mountainous province (central part of survey area)

SBP measurement was conducted during the movement among seamounts for cobalt crust survey, therefore the data in this region are insufficient for definitive consideration. Types b and e₁ are distributed in the valleys of the mountains and flat floor. They are of small scale. Type d₁ and ds are distributed in an intermittent manner. The intermountain sea-floor is relatively flat and it is inferred that turbidite deposits cover these zones.

iii) Quasi plain (eastern part of survey area)

The area 5°S - 8°S is mainly covered by types ds and d₁ material. Type e₁ is concentrated north of 5°S and in the southeastern part. In other parts of the province, the distribution of e₁ is small and intermittent. Type c mainly occurs around e₁ in the southeastern part. Type b is scattered in the northwest end of the province. Type d₂ occurs scattered north of 5°S.

3) The Distribution of the Upper Transparent Layers (Annexed Fig. 5)

The upper transparent layers occur in areas of SBP types b and e₁, thus the SBP type distribution map will be the basic reference material for the survey area. The thickness of types b and e₁ is 10~60 m, large portion is less than 40 m and the area of the upper transparent layer occurrence is limited. A fair size occurrence of 30~40 m thick, is observed to the south of approximately 6°45'S in the western part of the plain. Also that of 10~30 m thick is found to the northeast of the quasi plain. There are also small scattered occurrences of these transparent layers in the mountainous and quasi plain areas.

3-3 Bottom Materials

1) Classification

Bottom Materials are classified according to the criteria shown in Table 3-3-1. Quantitative analysis of each composition was made by the microscopic observation using smear slides (x100).

Table 3-3-1 Classification Standards of Bottom Materials

	Total Fossil (%)	Siliceous (*1) Fossil (%)	Calcareous (*2) Fossil (%)	Remarks
Brown clay	< 10			
Siliceous clay	10 ~ 30		< 5	
Silic-calcareous clay	10 ~ 30		> 5	Siliceous fossil > Calcareous fossil
Calc-siliceous clay	10 ~ 30	> 5		Calcareous fossil > Siliceous fossil
Calcareous clay	10 ~ 30	< 5		
Foraminifera ooze	> 30			Mainly foraminifera dominant
Silic-calcareous ooze	> 30		> 5	
Siliceous ooze	> 30		< 5	

*1 Radiolaria, Diatom, Silicoflagellate, Sponge spicule

*2 Foraminifera, calcareous nannoplankton

2) Distribution and Properties

i) Distribution

The ratio of bottom materials in the samples is shown in Table 3-3-2, and the distribution in Fig. 3-3-1. The bottom materials in the survey area are composed predominantly of brown clay which constitute 90% of the samples. Calcareous clay was collected at six localities of two stations in shallow waters near seamounts and knolls, these constitute 10% of the total samples. Old sediments were not observed during this survey. It is shown in the distribution map (Fig. 3-3-1) that brown clay occurs almost throughout the survey area, and calcareous material occurs at the topographic high near the 4,100~4,500 m deep zone of the seamounts at the southern fring of the eastern

sea. The spade corer sampling at five localities yielded brown and calcareous sediments from the surface, but old sediments were not encountered in the deeper (50 cm below surface at the deepest point) parts. Micro-nodules and volcanic glass were abundant in these parts.

Table 3-3-2 Sampling Ratio of Bottom Materials

Age	Classification	Sampling Number	Ratio (%)	
Quaternary	Brown clay	57	90	100
	Calcareous clay	6	10	

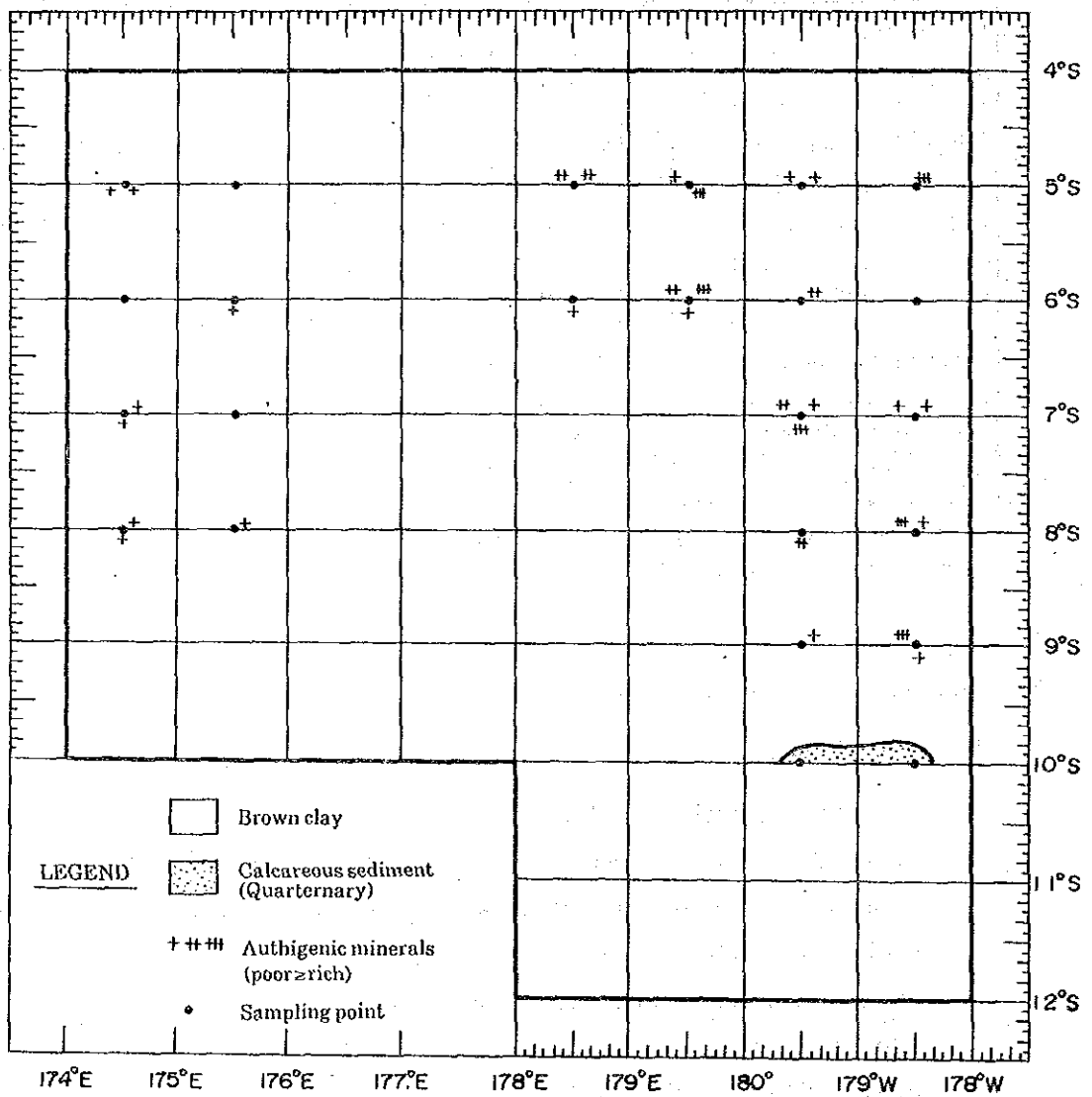
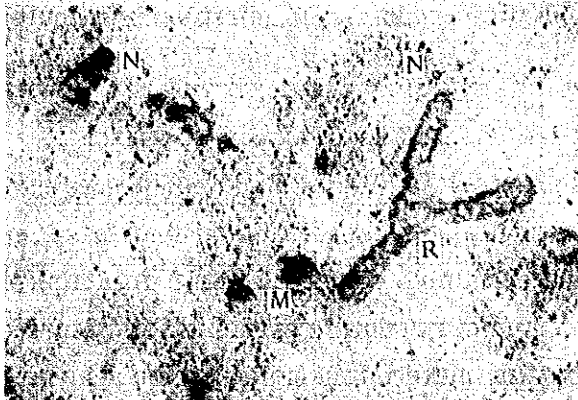


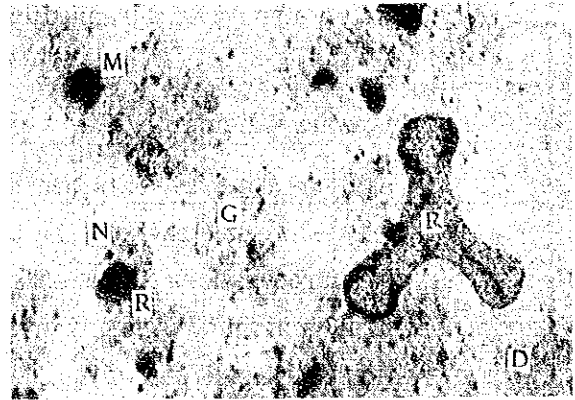
Figure 3-3-1 Distribution of Bottom Materials

ii) Properties

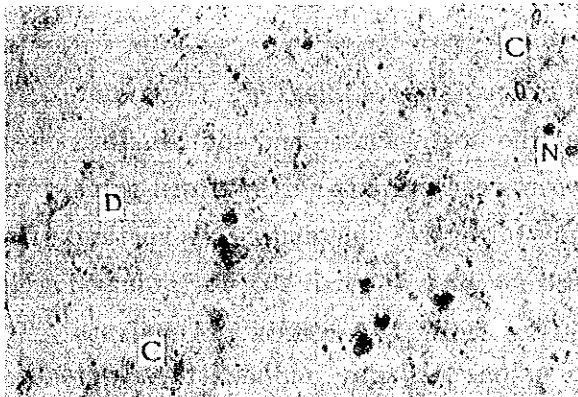
Fig. 3-3-2 shows the representative micrographs of the sediments. The general properties are described in this section.



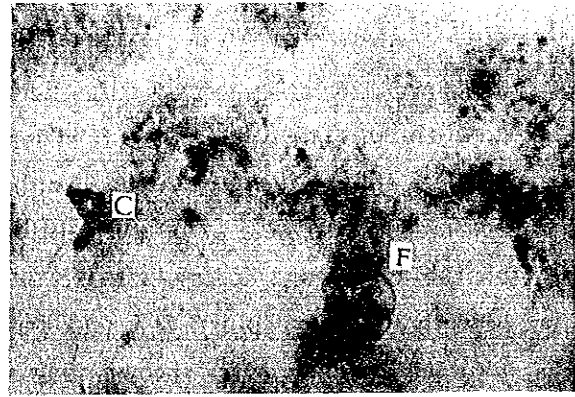
Brown clay (88S0679FG01)



Brown clay (88S0879SC01)



Calcareous clay (88S0875FG03)



Calcareous clay (88S1179FG03)

Legend

R : Radiolaria D : Diatom F : Foraminifera C : Carbonate
M : Mud fragment N : Micro-nodule G : Volcanic glass

Figure 3-3-2 Smear Slide Photos of Bottom Sediments

Brown clay

The main components of brown clay are clay minerals with small amount of micro-nodules, pyroclastic materials, ichthyolith, zeolites, etc. Characteristically, the bottom materials in the surveyed area contain large amount of pyroclastics and micro-nodules, 1% micro-nodule content is not rare.

Calcareous sediments

Calcareous sediments are classified by the content of calcareous shells and siliceous shells. In the survey area, only calcareous clay and calcareous ooze were observed. Mainly, they consist of foraminifera fragments and small amount of micro-nodules, pyroclastic materials, ichthyolith, zeolites, etc. The bottom materials sampled on the seamounts during the survey of cobalt crusts, were all coarse calcareous ooze. These sediments contain, aside from coarse foraminifera, large amount of micro-nodules and volcanic glass and they are generally medium-grained with rough texture.

3) Mineral Composition

Bottom material samples were collected by spade corer (SC) from five points. The localities are; two in the western sea, at the northeastern and southeastern parts, three in the eastern sea, at the southeastern, eastern and northeastern parts. Also box coring was done at four localities. Material was sampled every vertical 10cm of the cores and X-ray powder diffraction was carried out for mineralogical investigation. Table 3-3-3 and Fig. 3-3-3 show the results of analysis. The sediments consisted of brown clay and calcareous clay and quartz, plagioclase, gypsum. Clay minerals were in almost all samples. Clay minerals are illite, chlorite and montmorillonite. Halite is generally contained. 88S1179SC01 consists of calcareous clay and large amount of calcite occur down to 40 cm depth. The vertical change of mineral composition below the sea-floor (upper and lower layers by SC) is observed as follows. In sample 88S1179SC01, plagioclase occurs down to 20 cm below the sea-floor surface and it is lacking below 20 cm. On the other hand, clay minerals are lacking above 30 cm depth.

Difference in mineral composition is not observed in the spade corer samples by north-south nor east-west directions except for the occurrence of calcareous clay in 88S1179SC01, (88S0879SC01, 88S0975SC01 and 88S0675SC01 were collected in the southeastern, southwestern and northwestern parts respectively. Fig. 2-1).

Table 3-3-3 Results of X-ray Diffraction Analysis of Bottom Materials

No.	Sample No.	Depth	Silicate Minerals				Others	
			Plazioclase	Quartz	Phillipsite	Clay mineral**	Calcite	Halite
1	88S0879S01	0	•	•		•		•
2	"	10 cm	•	•		•		•
3	"	20 cm	•	•	?	•		•
4	"	30 cm	•	•		•		•
5	"	40 cm	•	•		•		•
6	"	50 cm	•	•		•		•
7	88S0975SC01	0	•	•		•		•
8	"	10 cm	•	•		•		•
9	"	20 cm	•	•		•		•
10	"	30 cm	•	•		•		•
11	"	40 cm	•	•		•		•
12	88S1179SC01	0	•	•			⊙	•
13	"	10 cm	?	•			⊙	•
14	"	20 cm		•			⊙	•
15	"	30 cm		•			⊙	•
16	"	40 cm		•		•	⊙	•
17	88S0675SC01	0	•	•		•		•
18	"	10 cm	•	•		•		•
19	"	20 cm	•	•		•		•

⊙ : Abundant • : Little ? : Uncertain

** Probably montmorillonite or illite/montmorillonite mixed layer mineral.

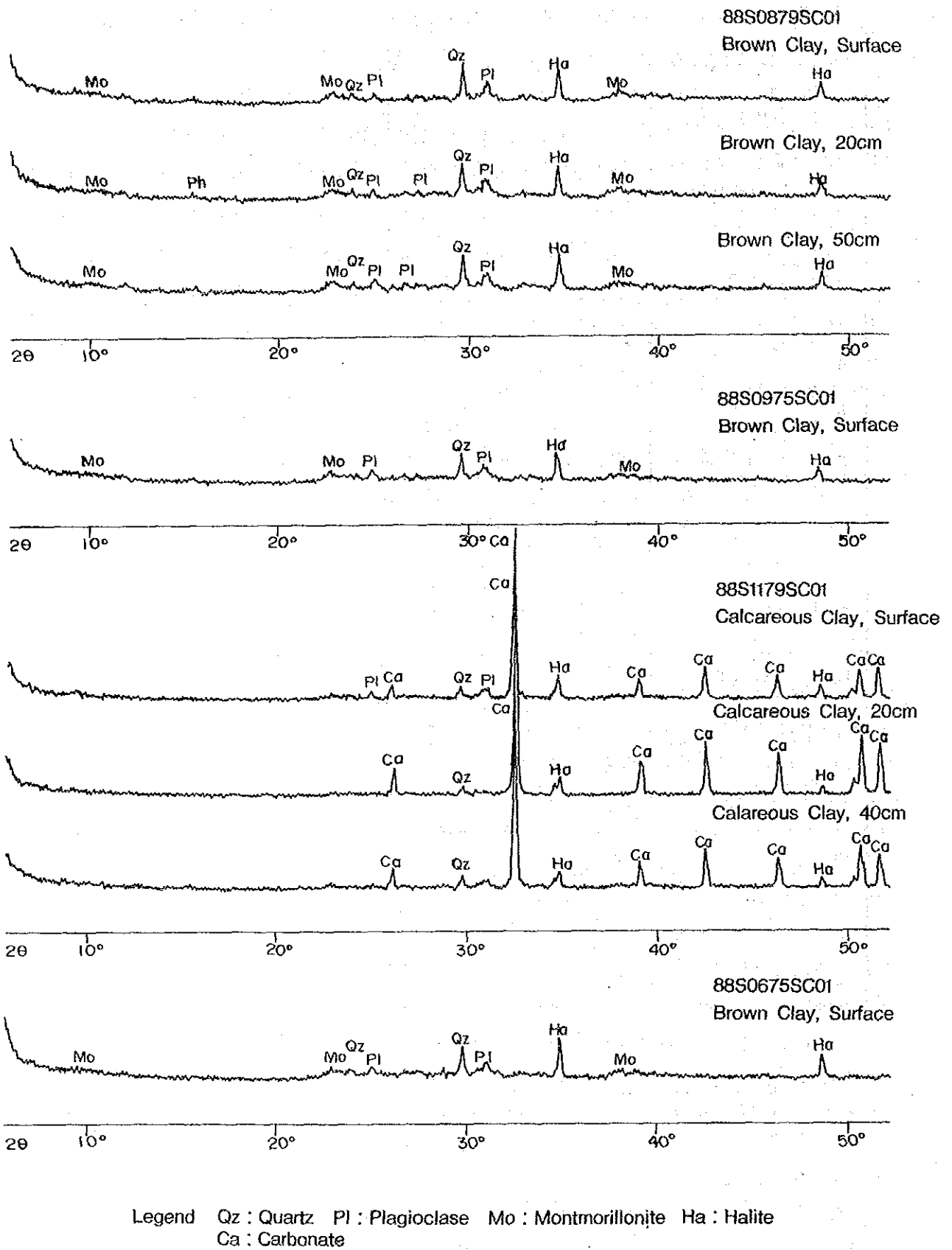


Figure 3-3-3 Typical X-ray Diffraction Patterns of Bottom Sediments

4) Chemical Composition

Material from the spade corer (SC) samples was taken every 10 cm from the surface and examined by chemical analysis. The results of the analysis are shown in Table 3-3-4. The following was clarified by this analysis on brown clay.

- i) Regarding the difference between the upper and lower layers, SiO_2 and TiO_2 show clear difference in content, but the behaviour is opposite in the eastern and western parts, namely in the eastern part SiO_2 is low and TiO_2 high in the upper layer whereas the relation is reverse in the west. BaO , Na_2O and P_2O_5 contents are nearly constant in both layers.
- ii) The contents of Al_2O_3 , Fe_2O_3 , FeO , MnO_2 , MgO , CaO vary between the two layers, but the trend of variation is not uniform.
- iii) The contents of SiO_2 , FeO , CaO , Na_2O , P_2O_5 and LOI are higher in the northern part (88S0675SC01) than in the southern part (88S0879SC01 and 88S0975SC01) while TiO_2 , Fe_2O_3 , MnO_2 , MgO , BaO and K_2O show the opposite behaviour. Al_2O_3 , however, show constant content throughout the area.
- iv) In comparing the western (88S0975SC01, 88S0675SC01) and the eastern (88S0879SC01) parts, the content of Al_2O_3 , FeO , CaO , P_2O_5 , LOI is higher in the western part while that of SiO_2 , TiO_2 , MnO_2 , MgO , BaO , Na_2O and K_2O has opposite trend. Fe_2O_3 content is nearly constant without significant differences.
- v) Compared with the chemical composition of DOMES Site-B*1. TiO_2 , Al_2O_3 , Fe_2O_3 , MgO , LOI contents are higher in the present area while SiO_2 , CaO , BaO and K_2O contents are lower.
- vi) The composition of calcareous clay (88S1179SC01) is higher in CaO and LOI but lower in all elements except FeO and BaO compared to brown clay. The content of all constituent elements vary in upper, middle and lower layers, but the trend of variation differs considerably.

*1 SiO_2 51.5%, TiO_2 0.59%, Al_2O_3 12.5%, Fe_2O_3 5.4%, MnO_2 0.53%, MgO 3.0%, CaO 1.5%, BaO 1.5%, Na_2O 5.7%, K_2O 3.3%, P_2O_5 0.51%, LOI 11.2% (Bischoff, J.L. et. al., 1979)

Table 3-3-4 Chemical Composition of the Bottom Materials

(%)

No.	Sample No.	Depth	Components and Values												
			SiO ₂ wt%	TiO ₂ wt%	Al ₂ O ₃ wt%	Fe ₂ O ₃ wt%	FeO wt%	MnO wt%	MgO wt%	CaO wt%	BaO wt%	Na ₂ O wt%	K ₂ O wt%	P ₂ O ₅ wt%	Loss wt%
1	88S0879SC01	Surface	44.35	1.02	14.74	9.34	0.28	1.21	3.77	2.35	0.17	4.85	2.03	0.47	14.54
2	"	10 cm	44.33	1.04	14.88	9.34	0.50	1.25	3.82	2.44	0.17	4.88	2.13	0.49	14.22
3	"	20 cm	44.39	1.00	15.00	9.55	0.13	1.24	3.71	2.21	0.15	4.90	2.19	0.46	14.08
4	"	30 cm	44.69	0.99	14.82	9.28	0.19	1.26	3.65	2.30	0.17	4.99	2.26	0.46	14.14
5	"	40 cm	45.82	0.93	14.46	8.81	0.30	1.17	3.51	2.26	0.18	4.86	2.16	0.46	14.16
6	"	50 cm	45.78	0.92	14.08	8.52	0.41	1.17	3.45	2.29	0.17	5.18	2.15	0.48	14.46
7	88S0975SC01	Surface	44.66	0.89	14.90	9.45	0.49	1.13	3.67	2.68	0.13	4.52	1.76	0.43	14.58
8	"	10 cm	45.09	0.87	14.75	9.36	0.35	1.15	3.64	2.53	0.13	4.73	1.73	0.42	14.38
9	"	20 cm	44.23	0.93	15.32	9.97	0.23	1.26	3.77	2.60	0.12	4.74	1.77	0.43	14.00
10	"	30 cm	43.09	0.99	15.91	10.57	0.18	1.36	3.53	2.71	0.11	4.64	1.73	0.44	13.67
11	"	40 cm	43.36	0.98	15.77	10.42	0.12	1.40	3.52	2.66	0.11	4.64	1.70	0.45	13.75
12	88S1179SC01	Surface	9.48	0.35	5.79	3.76	0.23	0.63	1.55	28.72	0.15	2.82	0.85	0.26	34.46
13	"	10 cm	14.79	0.24	4.32	2.10	0.55	0.43	1.19	35.45	0.13	2.45	0.70	0.18	36.87
14	"	20 cm	13.23	0.21	3.76	2.00	0.28	0.38	1.23	37.20	0.11	2.06	0.57	0.15	38.37
15	"	30 cm	11.93	0.20	3.37	2.07	0.13	0.38	0.99	37.96	0.10	1.93	0.53	0.17	39.73
16	"	40 cm	21.12	0.46	6.90	4.79	0.12	0.78	1.89	26.63	0.15	2.85	0.94	0.35	32.26
17	88S0675SC01	Surface	45.94	0.79	14.67	7.61	0.67	0.94	3.38	2.46	0.12	5.00	1.82	0.52	15.15
18	"	10 cm	45.76	0.83	15.28	8.06	0.50	1.13	3.45	2.40	0.12	4.96	1.98	0.52	14.49
19	"	20 cm	45.31	0.81	14.83	7.73	0.60	1.08	3.38	2.87	0.12	5.00	1.92	0.52	15.04

X	51.3	0.59	12.5	5.4	-	0.53	1.5	3.0	1.5	-	5.7	3.3	11.2
---	------	------	------	-----	---	------	-----	-----	-----	---	-----	-----	------

(%)

No.	Sample No.	Depth	Components and Values												Total wt%
			Pb ppm	V ppm	B ppm	Zn ppm	Y ppm	Ni ppm	Cu ppm	Co ppm	As ppm	Sr ppm	Mo ppm		
1	88S0879SC01	Surface	138	171	89	568	82	167	382	160	16	271	<1	99.12	
2	"	10 cm	122	172	94	668	85	176	398	160	15	282	<1	99.49	
3	"	20 cm	78	168	86	340	83	173	356	157	14	279	<1	99.01	
4	"	30 cm	78	167	89	304	83	175	356	163	12	274	<1	99.20	
5	"	40 cm	78	160	100	247	85	172	330	148	13	266	<1	99.08	
6	"	50 cm	78	160	96	278	86	167	328	145	11	265	<1	99.06	
7	88S0875SC01	Surface	81	186	90	334	82	201	373	146	12	252	<1	99.19	
8	"	10 cm	75	186	93	323	82	202	369	144	14	252	<1	99.13	
9	"	20 cm	75	196	88	243	86	205	403	151	16	256	<1	99.43	
10	"	30 cm	78	204	87	237	87	215	418	150	15	272	1	98.93	
11	"	40 cm	75	199	93	241	90	229	405	150	18	272	3	98.88	
12	88S1179SC01	Surface	60	72	44	198	52	100	188	81	7	1137	<1	89.05	
13	"	10 cm	52	49	30	112	41	82	147	76	7	1312	<1	99.40	
14	"	20 cm	47	41	25	157	41	74	123	84	4	1422	<1	99.55	
15	"	30 cm	44	39	28	146	40	70	125	78	4	1434	<1	99.49	
16	"	40 cm	62	87	50	137	74	117	201	96	7	1075	<1	99.24	
17	88S0675SC01	Surface	94	159	76	1068	99	182	352	136	14	252	<1	99.07	
18	"	10 cm	60	165	93	408	102	205	350	152	12	265	<1	99.48	
19	"	20 cm	57	159	74	172	103	186	339	146	13	271	<1	99.21	

X	-	0.17	-	-	-	-	-	-	-	-	-	-	-	-
---	---	------	---	---	---	---	---	---	---	---	---	---	---	---

No. 1~19 : Results of this survey
X : DOMES Site-B (Bischoff J.L. et al., 1979)

vii) The correlation coefficient of the constituent elements are shown in Table 3-3-5. It is seen that MnO₂ shows positive correlation with TiO₂, Fe₂O₃ and negative correlation with SiO₂, FeO, LOI. Fe₂O₃ correlates positively with V and Cu aside from MnO₂ and negatively with FeO, Na₂O, P₂O₅ and LOI. Ni correlates positively with Al₂O₃ and V and negatively with BaO and K₂O. Cu has positive correlation with Fe₂O₃ and V and negative correlation with SiO₂ and Na₂O. Also positive correlation is observed between P₂O₅ and Y, TiO₂ and Co.

Table 3-3-5 Correlations among Chemical Components of Bottom Materials

	SiO ₂	TiO ₂	Al ₂ O ₃	Fe ₂ O ₃	FeO	MnO ₂	MnO	CaO	Na ₂ O	Na ₂ O	K ₂ O	P ₂ O ₅	LOI	Pb	V	R	Zn	Y	Ki	Cu	Co	As	Sr	Ph
SiO ₂	1.00	-0.68	-0.78	-0.90	0.67	-0.84	-0.48	-0.37	0.29	0.66	0.35	0.55	0.73	-0.29	-0.92	-0.03	0.28	0.39	-0.51	-0.89	-0.44	-0.70	-0.40	-0.45
TiO ₂		1.00	0.22	0.73	-0.71	0.88	0.71	-0.32	0.48	-0.22	0.35	-0.49	-0.73	0.54	0.53	0.45	-0.17	-0.71	-0.15	0.51	0.19	0.42	0.68	0.19
Al ₂ O ₃			1.00	0.62	-0.44	0.62	0.09	0.53	-0.70	0.63	-0.57	-0.26	-0.58	-0.20	0.78	-0.11	-0.23	0.13	0.83	0.78	0.17	0.61	0.19	0.48
Fe ₂ O ₃				1.00	-0.82	0.89	0.59	0.13	-0.11	-0.72	-0.29	-0.82	-0.88	0.15	0.86	0.37	-0.40	-0.67	0.47	0.80	0.41	0.69	0.23	0.48
FeO					1.00	-0.85	-0.42	0.20	-0.10	0.35	-0.47	0.67	0.87	0.02	-0.53	-0.39	0.53	0.68	-0.21	-0.42	-0.52	-0.44	-0.38	-0.38
MnO ₂						1.00	0.44	0.88	0.80	-0.43	-0.84	-0.56	-0.93	0.66	0.67	0.44	-0.54	-0.48	0.39	0.66	0.59	0.53	0.55	-0.51
MnO							1.00	-0.25	0.36	-0.38	0.15	-0.54	-0.40	0.58	0.34	0.31	-0.80	-0.75	-0.13	0.52	0.68	0.35	0.23	-0.13
CaO								1.00	-0.76	-0.44	-0.76	-0.84	0.07	-0.31	0.51	-0.49	-0.24	0.41	0.67	0.44	-0.35	0.33	-0.18	0.28
Na ₂ O									1.00	0.45	0.85	0.03	-0.82	0.50	-0.55	0.48	0.06	-0.52	-0.84	-0.40	0.49	-0.32	0.39	-0.34
K ₂ O										1.00	0.68	0.71	0.46	-0.92	-0.84	-0.15	0.24	-0.37	-0.69	-0.71	0.81	-0.50	0.23	-0.34
P ₂ O ₅											1.00	0.32	0.94	0.21	-0.71	0.25	0.02	-0.19	-0.83	-0.55	1.55	-0.46	0.58	-0.36
LOI												1.00	0.64	0.01	-0.73	0.47	0.88	-0.25	-0.45	-0.12	-0.28	0.22	-0.15	
Pb													1.00	0.05	-0.67	-0.56	0.51	0.53	-0.48	-0.58	-0.47	-0.43	-0.41	-0.40
V														1.00	-0.06	0.11	0.58	-0.42	-0.44	0.32	0.39	0.37	0.24	-0.11
R															1.00	0.15	-0.34	-0.34	0.80	0.87	0.84	0.61	-0.12	0.43
Zn																1.00	-0.31	-0.55	-0.80	0.03	0.28	-0.06	0.10	0.16
Y																	1.00	0.21	-0.39	-0.81	-0.18	0.69	-0.17	-0.18
Ki																		1.00	0.29	-0.29	-0.42	-0.13	-0.68	0.87
Cu																			1.00	0.51	-0.25	0.45	-0.26	0.57
Co																				1.00	0.28	0.77	0.14	0.36
As																					1.00	0.17	0.74	-0.02
Sr																						1.00	0.19	0.68
Ph																							1.00	0.16

5) Authigenic Minerals

With a view to analyzing the components of authigenic minerals, X-ray powder diffraction was carried out. The results are shown in Table 3-3-6 and Fig. 3-3-4. Plagioclase, quartz, phillipsite, montmorillonite, fluorapatite, 10Å manganite and δ-MnO₂ were detected.

6) Carbonate Compensation Depth (CCD)

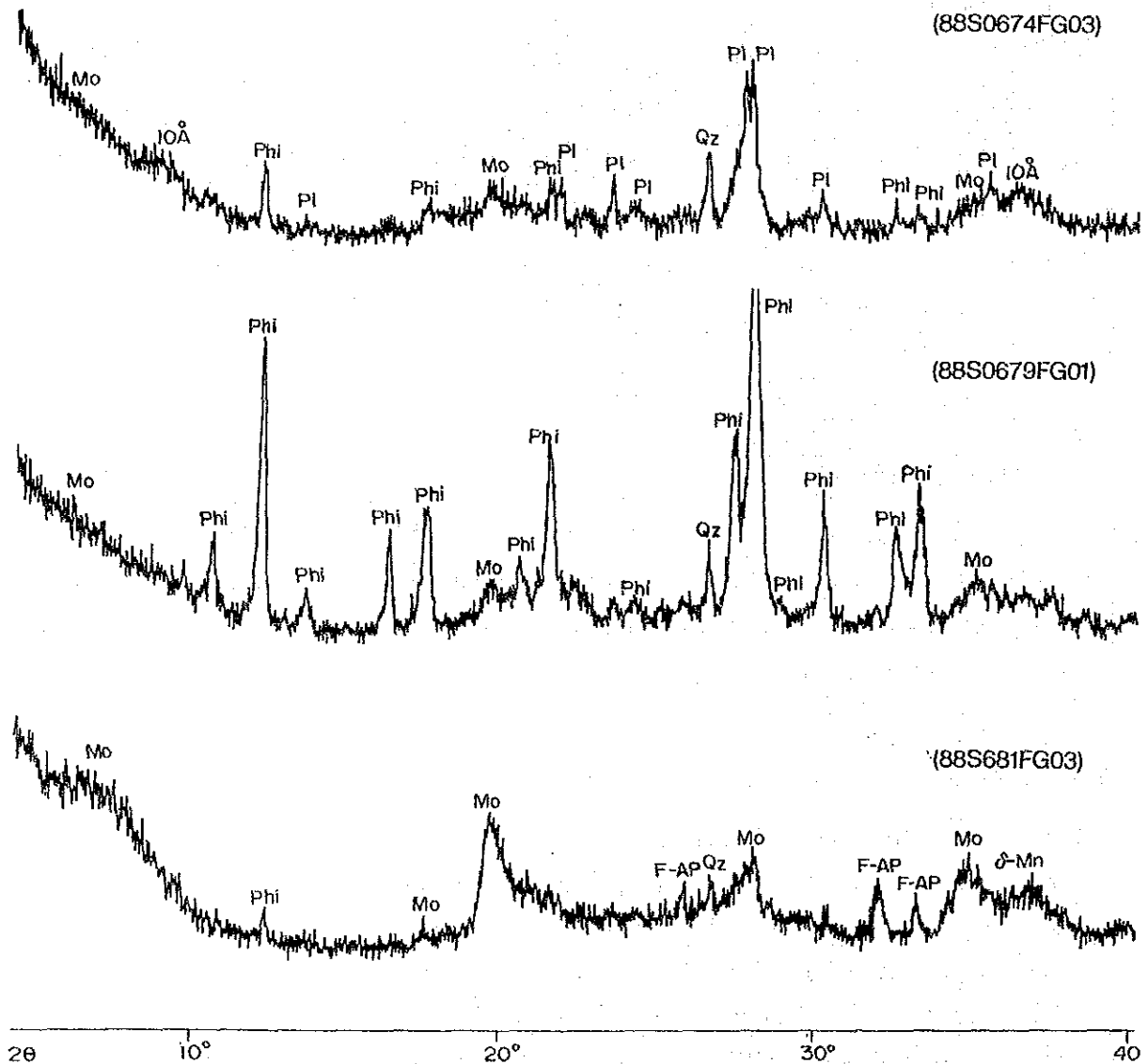
Data on calcareous surficial sediments are relatively few in the survey area. Microscopic study of smear slides confirmed that the maximum water depth for the existence of calcareous micro-fossils in surficial sediments is 4,827 m and the uppermost water depth for the extinction of carbonate minerals in the sediments is 5,031 m. Thus it is concluded that the maximum water depth in which carbonate minerals do not occur, CCD of the survey area is approximately 4,900 ~ 5,000 m.

Table 3-3-6 Results of X-ray Diffraction Analysis of Authigenic Minerals

	Mn-minerals		Siliceous minerals				Others
	10Å Mn	δ-Mn	Pl	Q	Phi	Mont	F·Ap
88S0674FG03	±		•	±	±	±	
88S0674FG03				±	⊙	?	
88S0674FG03		±		±		•	±

Legend

⊙ : Abundant ○ : Common • : Little ± : Very little ? : Obscure
 10Å Mn : 10Å Manganite, δ-Mn : δ-MnO₂, Pl : Plagioclase,
 Q : Quartz, Phi : Phillipsite, Mont : Montmorillonite,
 F·Ap : Fluorapatite



Legend 10Å : 10Å Manganite δ-Mn : δ-MnO₂ Qz : Quartz Pl : Plagioclase Mo : Montmorillonite
 Phi : Phillipsite F-AP : Fluor Apatite

Figure 3-3-4 Typical X-ray Diffraction Patterns of Authigenic Minerals

7) Paleontological Considerations

Through the study of fossils (Radiolaria, Foraminifera) in the surficial sediments sampled by spade corer, the age and sedimentary environment of the sea-floor were examined. Samples from three locations deeper than 40 cm below the sea-floor were used for the study.

(1) Radiolaria

i) Methods of investigation

Sixteen samples from 5, 10, 20, 30, 40 cm (and 50 cm) depth were selected on board from the three spade corer samples. These were processed as follows.

- a) Radiolaria was washed and concentrated by 2 μ m screen on land.
- b) Individuals were separated, washed and concentrated by ultrasonic cleaner.
- c) After drying under room temperature, individuals were separated under stereo-microscope.
- d) The extracted fossils were observed by scanning electron microscope, list of occurring radiolaria was prepared.

ii) Occurrence of fossils (Table 3-3-7, Fig. 3-3-5)

a) 88S0879SC01

Surface:

Sixty-one species, 41 genera were identified. A large number of individuals occur, preservation is good. Forty-six percent of the radiolaria has etched surfaces and over 45% have clear unetched surface.

10 cm:

Seventy-seven species, 57 genera were identified. A large number of individuals occur, preservation is very good. Forty-three percent of the radiolaria has somewhat etched surfaces and over 50% have clear unetched surface.

20 cm:

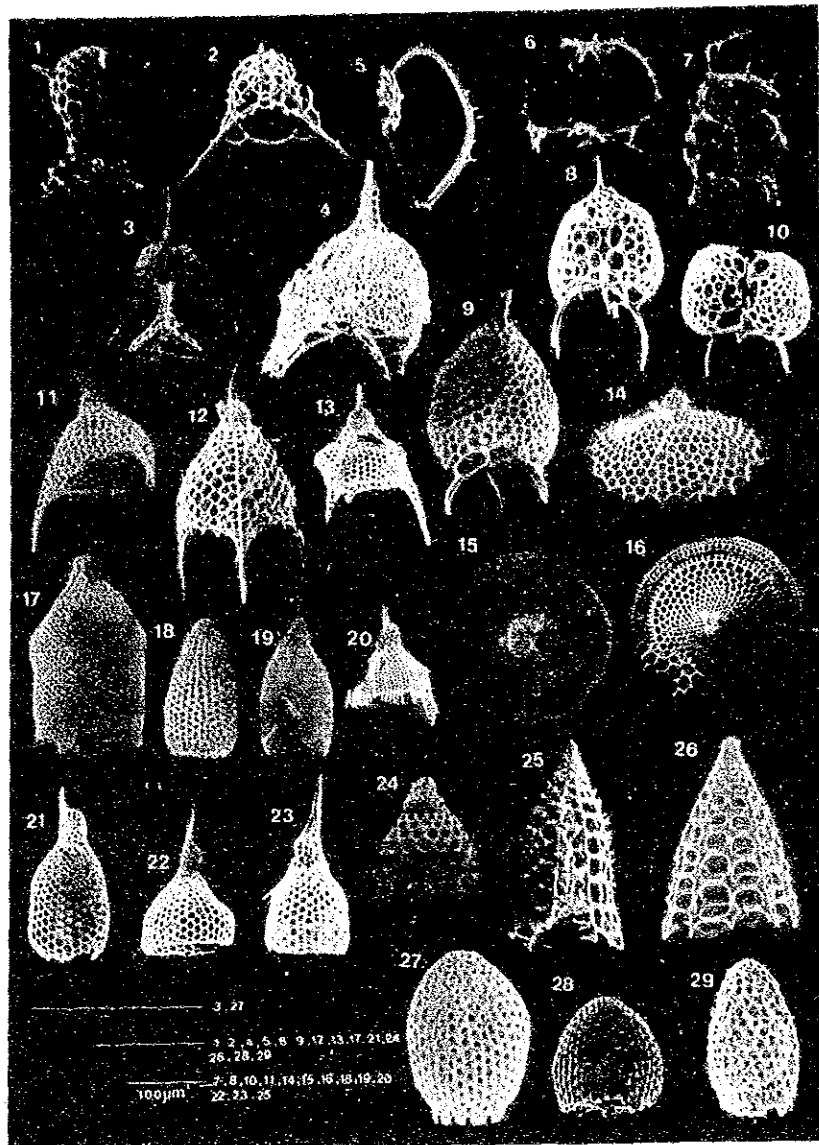
Sixty-four species, 41 genera were identified. A large number of individuals occur, preservation is not as good as the surface and

Table 3-3-7 List of Radiolarian Fossiles (1)

Radiolarian Species	88S0879SC01						88S0975SC01					88S1179SC01				
	Surface	10 cm	20 cm	30 cm	40 cm	50 cm	Surface	10 cm	20 cm	30 cm	40 cm	Surface	10 cm	20 cm	30 cm	40 cm
<i>Acrosphaera collina</i>	X	X											X			
<i>Acrosphaera cyrtodon</i>							X						X			
<i>Acrosphaera flammabunda</i>				X			X	X				X	X	X		X
<i>Acrosphaera lappacea</i>			X				X	X				X				X
<i>Acrosphaeramurrayana</i>		X	X					X						X		
<i>Acrosphaera spinosa</i>		X														X
<i>Buccinosphaera invaginata</i>	X	X					X	X		X		X	X			
<i>Collosphaera huxleyi</i>	X	X					X	X		X		X	X	X		
<i>Collosphaera tuberosa</i>	X	X	X				X	X	X	X		X	X	X		
<i>Disolenia quadrata</i>												X	X			
<i>Disolenia zanguebarica</i>	X		X					X	X			X	X	X		X
<i>Otosphaera auriculata</i>			X									X				X
<i>Otosphaera polymorpha</i>			X				X	X		X		X	X			
<i>Siphonosphaera martensi</i>	X	X	X					X				X	X			X
<i>Siphonosphaera socialis</i>		X	X					X		X		X				X
<i>Solenosphaera spp.</i>		X												X		
<i>Acanthosphaera capillaris</i>	X						X	X		X		X				
<i>Acanthosphaera castanea</i>								X				X				
<i>Acanthosphaera minuta</i>							X					X				
<i>Actionomma archadophorum</i>							X					X				
<i>Actionomma mediterraneensis</i>							X					X				
<i>Actionomma sp.</i>	X	X		X			X	X				X				
<i>Actionosphaera heckeli</i>		X					X	X					X			X
<i>Amphisphaera palliatum</i>		X					X	X				X	X			X
<i>Centroculus cladostylus</i>		X					X						X			X
<i>Druppatractus ostracion</i>		X						X								
<i>Hexacontium anaximandri</i>	X		X	X			X	X	X	X		X	X	X	X	X
<i>Hexacontium arachnoidale</i>	X		X	X			X	X				X				X
<i>Hexacontium asterocanthion</i>								X				X				
<i>Hexacontium axotrias</i>							X					X				
<i>Hexacontium favosum</i>		X						X		X		X			X	X
<i>Hexacontium heracliti</i>	X						X			X		X				
<i>Hexacontium hostile</i>	X				X			X				X				
<i>Prunopyle antarctica</i>	X	X	X	X			X	X	X			X	X	X	X	
<i>Prunopyle hayesi</i>	X	X	X				X	X				X				
<i>Rhizosphaera serrata</i>		X					X	X				X				
<i>Stylatractus melpomene</i>	X		X				X	X				X	X	X		
<i>Stylatractus neptunus</i>		X					X	X				X	X	X		
<i>Stylatractus sp.</i>		X	X									X				
<i>Xipholatractus sp.</i>	X	X	X	X	X	X	X	X	X	X		X	X	X	X	X
<i>Ommatarus tetrathalamus</i>	X	X	X	X	X		X	X	X	X		X	X	X		X
<i>Heliodiscus asteriscus</i>	X	X	X						X			X	X	X		X
<i>Heliodiscus ochiniscus</i>	X	X	X				X		X			X			X	X
<i>Euchitonia elegans</i>	X	X	X	X	X		X			X		X	X	X	X	X
<i>Euchitonia furcata</i>		X	X	X			X					X	X			X
<i>Dictyocoryne profunda</i>	X	X	X	X			X	X	X			X	X	X	X	X
<i>Dictyocoryne truncatum</i>	X	X	X	X			X	X	X	X		X	X	X	X	X
<i>Spongaster tetras tetras</i>	X	X	X	X			X	X	X			X	X		X	
<i>Spongaster tetras irregularis</i>	X		X				X	X				X				
<i>Spongodiscus biconcavus</i>	X		X		X		X	X	X				X	X		X
<i>Spongodiscus osculosus</i>	X	X	X	X			X	X	X	X		X	X	X	X	X
<i>Spongocore cylindrica</i>		X					X	X				X	X	X		
<i>Eueccryphus sesterodiscus</i>		X														
<i>Plegmosphaera lepticali</i>		X					X	X								
<i>Tessarastrum staussii</i>		X					X									
<i>Tetrapyle octacantha</i>	X	X		X	X		X	X		X		X	X	X	X	X
<i>Lithomelissa butschlii</i>	X	X	X		X											
<i>Lithomelissa sp.</i>	X	X	X					X		X		X				
<i>Lophosphaena hispida</i>	X	X	X	X						X						
<i>Peridium longispinum</i>	X	X														
<i>Pseudodictyophimus spp.</i>												X				
<i>Psilomelissa sp.</i>								X				X				
<i>Dictyophimus crisisae</i>							X					X				
<i>Dictyophimus playcephalus</i>												X				
<i>Ceratocyrtis sp.</i>	X	X	X						X							
<i>Lampromitra coronata</i>			X				X					X				

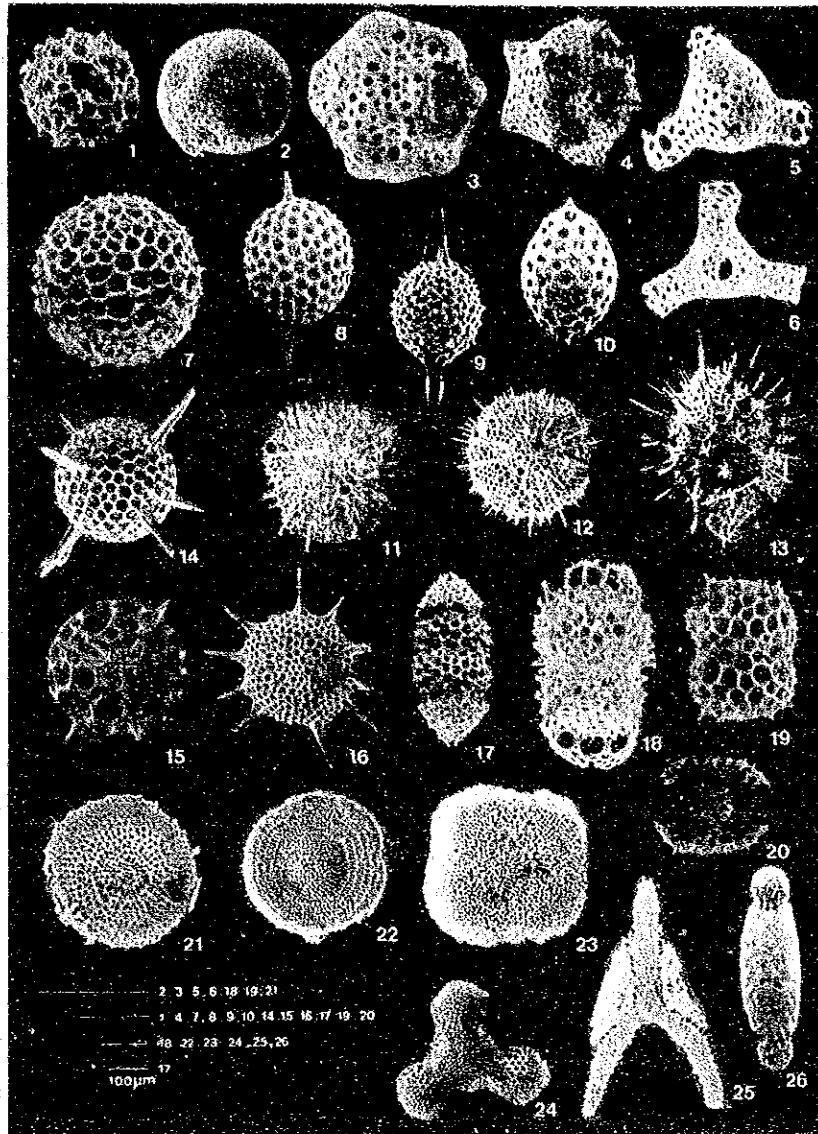
Table 3-3-7 List of Radiolarian Fossiles (2)

Radiolarian Species	Samples	88S0879SC01					88S0975SC01					88S1179SC01					
		Surface	10 cm	20 cm	30 cm	40 cm	50 cm	Surface	10 cm	20 cm	30 cm	40 cm	Surface	10 cm	20 cm	30 cm	40 cm
Lampromitra quadricuspis		X	X	X			X					X	X				
Archipilium sp.												X					
Cladoscenium pectinatum			X														
Clathrocanium diadema			X									X					
Clathrocanium triomma			X														
Clathromitra pentacantha			X														
Plectoscenium eucolpium			X														
Verticillata pinnatum			X														
Zygocircus productus productus		X	X	X			X	X	X			X			X	X	
Acanthodesmia vinculata group		X	X	X	X	X	X	X	X	X		X	X	X	X	X	
Liriospyris reticulata		X	X	X		X	X	X		X		X	X	X	X	X	
Lophospyris pentagona hyperborea							X	X	X			X					
Lophospyris pentagona pentagona				X			X	X				X					
Nephrospyris renilla			X											X			
Tholospyris acuminata		X	X	X		X	X	X	X			X	X				
Tholospyris baconiana variabilis		X	X	X				X									
Tholospyris scaphipes		X	X					X									
Tholospyris spp.		X					X	X				X	X				
Triospyris angulata				X													
Sethoconus cosinodiscus			X														
Tripoconus sp.		X	X	X													
Theocalyptra bicornis		X	X					X	X			X		X	X	X	
Eucyrtidium acuminatum		X	X					X	X	X	X	X	X				
Eucyrtidium anomalum		X	X					X	X			X					
Eucyrtidium dictyopodium		X						X	X			X					
Eucyrtidium hexagonatum			X	X			X	X				X	X				
Eucyrtidium hexastium							X			X							
Lipmanella pyramidale		X		X				X				X					
Lithopera bacca		X	X	X	X				X			X					
Pterocanium praetextum praetextum		X	X	X			X	X		X		X					X
Pterocanium trilobum		X	X	X	X		X	X	X			X	X	X			X
Pterocanium virgentum		X	X	X			X	X				X					X
Anthocyrtidium ophirensis		X	X	X	X		X	X	X	X		X	X	X		X	X
Anthocyrtidium zanguebaricum		X	X	X	X	X	X	X	X			X	X	X	X	X	X
Lamprocyclus maritilis maritilis		X	X	X			X	X	X	X		X	X				X
Lamprocyclus neoheteroporus		X	X	X	X		X	X					X				X
Lamprocyrtis nigrinae		X	X	X			X	X	X	X			X				X
Pterocorys hertwigi		X	X	X			X										X
Pterocorys zancleus		X	X	X	X	X	X	X	X				X	X	X	X	X
Theocorythium trachelium trachelium		X	X	X		X	X					X	X				X
Botryostrobus aquilonalis				X	X		X	X	X	X		X					X
Botryostrobus auritus				X			X	X	X			X		X			X
Lithocampe heptacola																	
Siphonocampe ercosa			X														
Tricolocampe sp.			X	X	X	X	X	X		X		X		X			
Carpocanistrum acidentata			X	X	X		X	X	X	X		X	X	X			X
Carpocanistrum coronatum			X	X			X	X				X					X
Carpocanistrum spp.			X	X			X	X	X			X		X	X	X	X
Spongocanium sp.			X	X			X		X			X					
Botryocyrti scutum								X				X					
Neobotrys quadritubulosa								X									
Bathropyramis circumtexta		X	X	X			X	X	X			X	X	X	X	X	X
Cornutella bimarginata		X	X	X			X	X				X	X	X			X
Cornutella profunda			X	X	X		X	X	X					X			X



- | | |
|--|---|
| 1. <i>Lithomelissa</i> sp. | 15. <i>Lampromitra coronata</i> Haeckel |
| 2. <i>Plectoscenium eucolpium</i> (Haeckel) | 16. <i>Eucecryphalus sestrodiscus</i> (Haeckel) |
| 3. <i>Clathrocanium triomma</i> Haeckel | 17. <i>Eucyrtidium anomalum</i> (Haeckel) |
| 4. <i>Verticillata pinnatum</i> (Haeckel) | 18. <i>Lithocampe heptacola</i> Haeckel |
| 5. <i>Zigocircus productus productus</i> Goll | 19. <i>Eucyrtidium hexagonatum</i> Haeckel |
| 6. <i>Acanthodesmia vinculata</i> (Muller) | 20. <i>Pterocorys hertwigi</i> (Haeckel) |
| 7. <i>Liriospyris reticulata</i> (Ehrenberg) | 21. <i>Anthocyrtidium zanguebaricum</i> (Ehrenberg) |
| 8. <i>Tholospyris acuminata</i> (Hertwig) | 22. <i>Anthocyrtidium ophirensis</i> (Ehrenberg) |
| 9. <i>Tholospyris</i> sp. | 23. <i>Lamprocyclas maritima maritima</i> Haeckel |
| 10. <i>Tholospyris</i> sp. | 24. <i>Theocaliptera bicornis</i> (Ehrenberg) |
| 11. <i>Pterocanium trilobum</i> (Haeckel) | 25, 26. <i>Bathropyramis circumtexta</i> (Haeckel) |
| 12. <i>Pterocanium</i> ps. | 27, 28. <i>Carpocanistrum acuminatum</i> Takahashi |
| 13. <i>Pterocanium praetextum</i> Praetextum (Ehrenberg) | 29. <i>Tricolocampe</i> sp. |
| 14. <i>Lampromitra quadricuspis</i> Haeckel | |

Figure 3-3-5 Species of the Typical Radiolarian Fossils (2)



- | | |
|---|--|
| 1. <i>Acrosphaera lappacea</i> (Haeckel) | 14. <i>Hexacontium anaximandri</i> Haeckel |
| 2. <i>Buccinosphaera invaginata</i> Haeckel | 15. <i>Hexacontium arachnoidale</i> Hollande et Enjunet |
| 3. <i>Collosphaera tuberosa</i> Haeckel | 16. <i>Heliodiscus asteriscus</i> Haeckel |
| 4. <i>Acrosphaera collina</i> (Haeckel) | 17-19. <i>Ommatartus tetrathalamus tetrathalamus</i> (Haeckel) |
| 5, 6. <i>Solenosphaera</i> spp. | 20. <i>Tetrapyle octacantha</i> Muller |
| 7. <i>Acanthosphaera capillaris</i> Haeckel | 21. <i>Pododiscus</i> (?) sp. |
| 8. <i>Amphisphaera palliatum</i> (Haeckel) | 22. <i>Stylodictya</i> sp. |
| 9. <i>Stylatractus neptunus</i> Haeckel | 23. <i>Spongaster tetras tetras</i> Ehrenberg |
| 10. <i>Xiphatractus</i> sp. | 24. <i>Dictyocoryne truncatum</i> (Ehrenberg) |
| 11. <i>Centrocubus cladostylus</i> Haeckel | 25. <i>Euchitonia elegans</i> (Ehrenberg) |
| 12. <i>Rhizosphaera serrata</i> Haeckel | 26. <i>Spongocore cylindrica</i> (Haeckel) |
| 13. <i>Prunopyle</i> sp. | |

Figure 3-3-5 Species of the Typical Radiolarian Fossils (1)

10cm material. Twenty-nine percent is completely unetched while 54% have etched surfaces and 17% have their septums strongly dissolved.

30 cm:

Twenty-nine species, 22 genera were identified. Relatively large number of individuals occur, but the number of species are limited compared to those of the upper layers.

Preservation is not good. There are 65% with surface etched and 16% with septums dissolved.

40 cm:

Fourteen species, 14 genera were identified. The number of occurring individuals is small and preservation is not good. There are 55% with surface etched somewhat and 30% with septum dissolved.

50 cm:

One species, one genus was identified. Very small number of individuals occur and preservation is bad.

b) 88S0975SC01

The surface:

Sixty-nine species, 41 genera were identified. A very large number of individuals occur and preservation is good. Forty-eight percent of the individuals are completely unetched. Twenty-nine percent has etched surfaces.

10 cm:

Sixty-four species, 46 genera were identified. A large number of individuals occur and preservation is relatively good. Forty-two percent is completely unetched. Those with etched surface amount to 37%.

20 cm:

Thirty-eight species, 28 genera were identified. Small number of individuals occur and preservation is bad. Unetched individuals are 17% and those with dissolved septum amount to 39%.

30 cm:

Twenty-nine species, 25 genera were identified. The number of individuals and species are small and preservation is bad. Unetched individuals are less than 15% of the total and those with dissolved septum amount to 33%.

40 cm:

Three species, three genera were identified. The number of individuals and species are very small and preservation is very bad. Completely unetched individuals are less than 2% of the total population. Over 66% has their septum dissolved.

c) 88S1179SC01

The surface:

Seventy-nine species, 48 genera were identified. A large number of individuals occur and preservation is good. Thirty-four percent are completely unetched, 30% are etched.

10 cm:

Forty-four species, 44 genera were identified. Very large amount of individuals occur and preservation is very good. Sixty-five percent of the radiolaria is completely unetched and only 8% has dissolved septum.

20 cm:

Thirty-seven species, 29 genera were identified. A large number of individuals occur and preservation is good. Unetched individuals are 59%. Fourteen percent has etched surfaces.

30 cm:

Nineteen species, 17 genera were identified. A large number of individuals occur and preservation is good. Unetched individuals are 54%. Twenty-four percent has etched surfaces.

40 cm:

Forty-five species, 29 genera were identified. A large amount of individuals occur and preservation is good. Unetched individuals are 50% and 24% are etched.

iii) Geologic age

The three samples (88S0879SC01), (88S0975SC01) and (88S1179SC01) all contain Recent radiolaria. *Collosphaera tuberosa* which appeared in Late Quaternary (approximately 400,000 years ago) and *Buccinosphaera invaginata* which appeared approximately 200,000 years back, occur below 30 cm in (88S0879SC01) and other samples except (88S0975SC01) which have very poorly preserved fossils at 40 cm and the age cannot be determined. *Solenisphaera* spp occurs in (88S0879SC01) 10 cm and (88S1178SC01) 20 cm. Of these species, those shown in 6 of Fig. 3-3-5 are very close to *Solenosphaera omnitubus* and are usually treated as the same species. *S. omnitubus* which indicates Late Miocene to Early Pliocene, however, have six to eight tubes according to the illustrations of Riedel et al. The number of tubes is larger than that of the present samples and is considered to be of different species. Also the individuals of the present samples are well preserved and is not considered to be redeposited material. Therefore, the *S. sp.* of the plate is treated as Recent species.

iv) Sedimentation rate

The sedimentation rate is calculated to be, over 0.5mm/1,000y from the occurrence of *Buccinosphaera invaginata* in (88S0879SC01), over 1.5mm/1,000y from (88S0975SC01), over 0.5mm/1000y from (88S1179SC01). The upper limit of the rate cannot be calculated because the position of the appearance of the same species cannot be identified.

v) Paleo-environment

The radiolaria which occur in these samples are those which generally live in the equatorial Pacific area and meaningful difference of constituent species are not observed among different samples. Various species such as *Eucyrtidium hertwigi*, *Eucytonia elegans* which are seen in the shallow sea of low latitude areas, *Clathrocanium* and *Pterocorys* which live in 100~200 m depth near the equator were confirmed. Species living in 200~1,000 m of water depth such as *Bathropyramis* also occur. All shallow to deep sea fauna occur in samples with non predominating. Therefore, these sediments are believed to have deposited in relatively quiet, deeper than 200 m sea-floor where the effect of current is not strong. Particularly, as (88S1179SC01) contains large amount of both planktonic and benthic foraminifera as well as radiolaria, it may have deposited in shallower waters than other two samples. Also as many of the larger

planktonic foraminifera have been destroyed, the environment could have been such that was easily affected by physical action. But the number of samples was so small that the determination of the age from radiolaria was not possible.

(2) Foraminifera

i) Method of investigation

The three spade corer samples were divided by inserting a plastic tubes of 6 cm diameter and 50 cm long into the samples on board. Then the tubes were cut vertically by an electric saw in the laboratory on shore. The core in the tube was cut vertically into two portions by a knife. One of the halves of the three samples were further separated into three parts, a total of nine parts by depth, surface~15 cm, 15~30 cm, 30~45 cm.

- a) Samples were screened by 200 (0.074 mm) sieve and washed.
- b) Dried under room temperature.
- c) Samples were separated from grains over #115 (0.125 mm) so that each batch contained more than 200 individuals of planktonic foraminifera and they were identified.
- d) Counted the benthic foraminifera which occur in these sediments and calculated the planktonic ratio (planktonic species \times 100/planktonic and benthic species).
- e) Benthic species were also extracted to over 200 individuals and identified the species.

ii) Occurrence (Table 3-3-8, Fig. 3-3-6)

All nine samples studied contained foraminifera fossils. In sample Nos. 1~6, planktonic species were lacking and only a minor amount of agglutinated benthic species were found. In sample Nos. 7~9, fossils were abundant and a very large amount of planktonic fossils were found. The benthic species were those living in deep sea and the planktonic species were those of tropical seas. Many of the planktonic type are damaged and planktonic ratio here is smaller than the impression from microscopic observation. The occurrence of foraminifera fossils in each sample is as follows.

88S0975SC01 upper·middle·lower (Nos. 1~3)

Only a small amount of agglutinated benthic foraminifera fossils

Table 3-3-8 List of Foraminifera Fossiles

Number	Sample Number								
	1	2	3	4	5	6	7	8	9
Sample Number	(Depth, cm)								
	88S0975SC01								
Agglutinated Foraminifers	0-15	15-30	30-45	0-15	15-30	30-45	0-15	15-30	30-45
	88S1179S01								
Rhabdammina abyssorum Sars	2			2					
Hyperammina cf. subnodosa Brady	2								
Reophax cf. nodulosus Brady				1		2			
Reophax sp.				2					
Oribostomoides sp.	1						2		
Haplophragmoides sp.							+		
Trochammina globigeriniformis (Parker & Jones)							2		
Trochammina sp.		1		2	1				
Recurvoides sp.	5	3		5	3		+	1	4
Eggerella bradyi nitens (Wiesner)							3	4	14
Siphotextularia sp.								2	4
Ammonassilina aveliniformis (Millett)	1								
unknown		1	1		2				2
Quinqueloculina spp.							1	1	1
Pyrgo murbinia (Schwager)							3	3	1
Dentalina sp.							1		
Lagena laevis Montagu							1		
Lagena nodulosa Cushman									
Lagena subformosa Parr									
Lagena spp.									
Oolina sulcata (Walker & Jacob)									
Oolina spp.							2	1	3
Fissurina fimbriata (Brady)							1		
Fissurina longispina (Brady)							3	3	2
Fissurina marginata Montagu							1		
Fissurina orbignyana Seguenza							2	2	2
Fissurina sp.							1	6	4
Fissurina spp.							1	2	
Lenticulina sp.								1	
Globobulimina sp.									
Fusenkoia fusiformis (Williamson)							1		
Pullenia aperta Cushman							4	9	7
Pullenia bulloides (d'Orbigny)							11	12	13
Pullenia spp.							2	3	6
Sphaeroidina bulloides d'Orbigny							1		
Chilostomella oolina Schwager							1	1	
Globocassidulina subglobosa Brady							4	6	5
Favocassidulina favus (Brady)							6	7	19
Cassidulinoides sp.									
Ehrenbergina sp.							2	2	2
Epistominella exigua (Brady)							109	54	23
Epistominella cf. exigua (Brady)							10	3	2
Epistominella sp. (young form)							46	64	11
Epistominella umboniferus (Natland)							29	24	51
Epistominella cf. umboniferus (Natland)							1		
Cibicides pseudoungerianus (Cushman)							9	19	10
Cibicides cf. pseudoungerianus (Cushman)							2		7
Eponides bradyi Earland							3	4	12
Eponides cf. turpidulus (Brady)									
"Nuttallides" cf. rugosa (Pfleger & Parker)							2		
Oridossalis tenerus (Brady)									
Oridossalis cf. umbonatus (Reuss)									
Gyroidina orbicularis d'Orbigny							1		2
Gyroidina soldanii d'Orbigny							4	1	6
Gyroidina spp.							4	2	4
Melonis pompilioides (Fichtel & Moll)							6	4	4
Melonis spp.							2	2	4
Total Agglutinated Foraminifers	11	5	1	12	6	2	7	8	23
Total Calcareous Porcellaneous Foraminifers	0	0	0	0	0	0	4	4	2
Total Calcareous Hyaline Foraminifers	0	0	0	0	0	0	273	246	216
Total Benthonic Foraminifers	11	5	1	12	6	2	234	258	248
Planktonic Foraminifer							10	14	36
Globigerinella nequilateralis (Brady)							1	1	1
Globigerinella calida (Parker)							1	1	1
Evella digitata (Brady)									
Globigerina bulloides d'Orbigny									
Globigerina falconensis Blow							1	1	5
G. lobigerina spp.							21	20	17
Globigerinoides conglobatus (Brady)							14	6	8
Globigerinoides quadrilobatus (d'Orbigny)							6	7	33
Globigerinoides sacculifer (Brady)							8	2	9
Globigerinoides ruber (d'Orbigny)									
Globigerinoides cf. extremus Bolli							1		1
Globigerinoides cf. obliquus Bolli							7	2	1
Ovulina univulsa (d'Orbigny)							2	6	5
Sphaeroidinella dehiscens (Parker & Jones)									
Sphaeroidinella sp.							1	+	
Candaina nitida d'Orbigny									
Globigerinita glutinata (Egger)							25	65	43
Pulleniatina obliquolucata (Parker & Jones) 右卷							2	3	
Pulleniatina cf. finalis Banner & Blow							44	45	46
Neoglobobulimina duterrei (d'Orbigny)							1	1	2
Neoglobobulimina spp.							2	4	2
Globorotalia crassaformis (Galloway & Wissler)							4	3	
Globorotalia crassa Cushman & Stewart							15	25	18
Globorotalia menardii (Parker, Jones & Brady)							3	1	2
Globorotalia scitula (Brady)							1	+	
Globorotalia truncatulinoides (d'Orbigny)							38	47	31
Globorotalia tumida (Brady)							203	254	272
Total Planktonic Foraminifers	0	0	0	0	0	0	0	254	272

occurs in this sample. There are no planktonic species. The benthic species which occur are *Rabdammina abyssorum*, *Recurvoides* sp. In sample No. 1, *Ammomassilina alveoliniformis* occur. The population not containing these calcareous fossils and consisting entirely of agglutinated material occur below the CCD.

88S0879SC01 (Nos. 4~6)

Only a small amount of agglutinated benthic foraminifera fossils occurs in this sample. There are no planktonic species. The benthic species are *Rabdammina abyssorum*, *Reophax* sp., *Trochamnina* sp., *Trecurvoides* sp. The population not containing these calcareous fossils and consisting entirely of agglutinated material occur below the CCD.

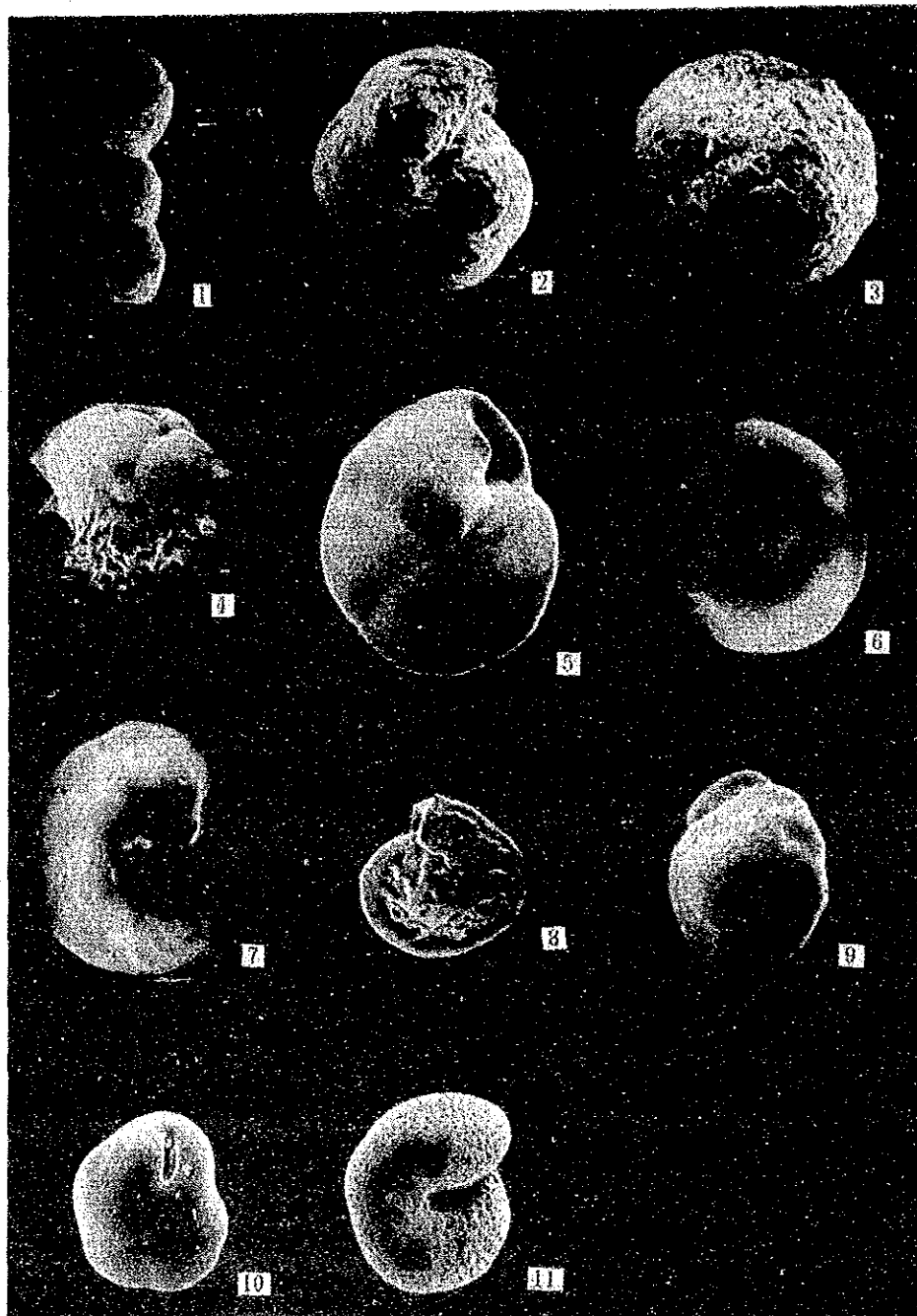
88S1179SC01 (Nos. 7~9)

Large amount of foraminifera fossils occur in this sample, most of the sand grains are foraminifera sands. The planktonic ratio is very high at over 90%. Deep sea benthic species *Epistominella exiqua*, *Epistominella umbonifarus* are abundant associated with *Fissurina* sp., *Pullenia* sp., *Cibicides pseudoungerianus*, *Melonis pompilioides*. The composition of the fossils do not vary significantly vertically, *E. exiqua* decreases downward while *Eggerella bradyi niteus*, *Favocassidulina favus*, *E. umboniferous* and *Eponides bradyi* increase. The mode of occurrence of planktonic species also do not vary vertically in the core. *Pulleniatina oblicuiloculata*, *Neogloboguadrina dutertrei*, *Globorotalia tumida* are abundant and associated with *Globigerinella aequilateralis*, *Globigerinoides conglobatus*, *Globigerinoides sacculifer* (s.l) and *Globorotalia menardii*. These are tropical marine population. *Globorotalia truncatulinoides* which is the indicator for Quaternary occurs from all samples together with *Beella digitata*, *Globigerinella calida* which occur in Quaternary units. *Pulleniatina oblicuiloculata* of this age are all sinistral.

iii) Geologic age

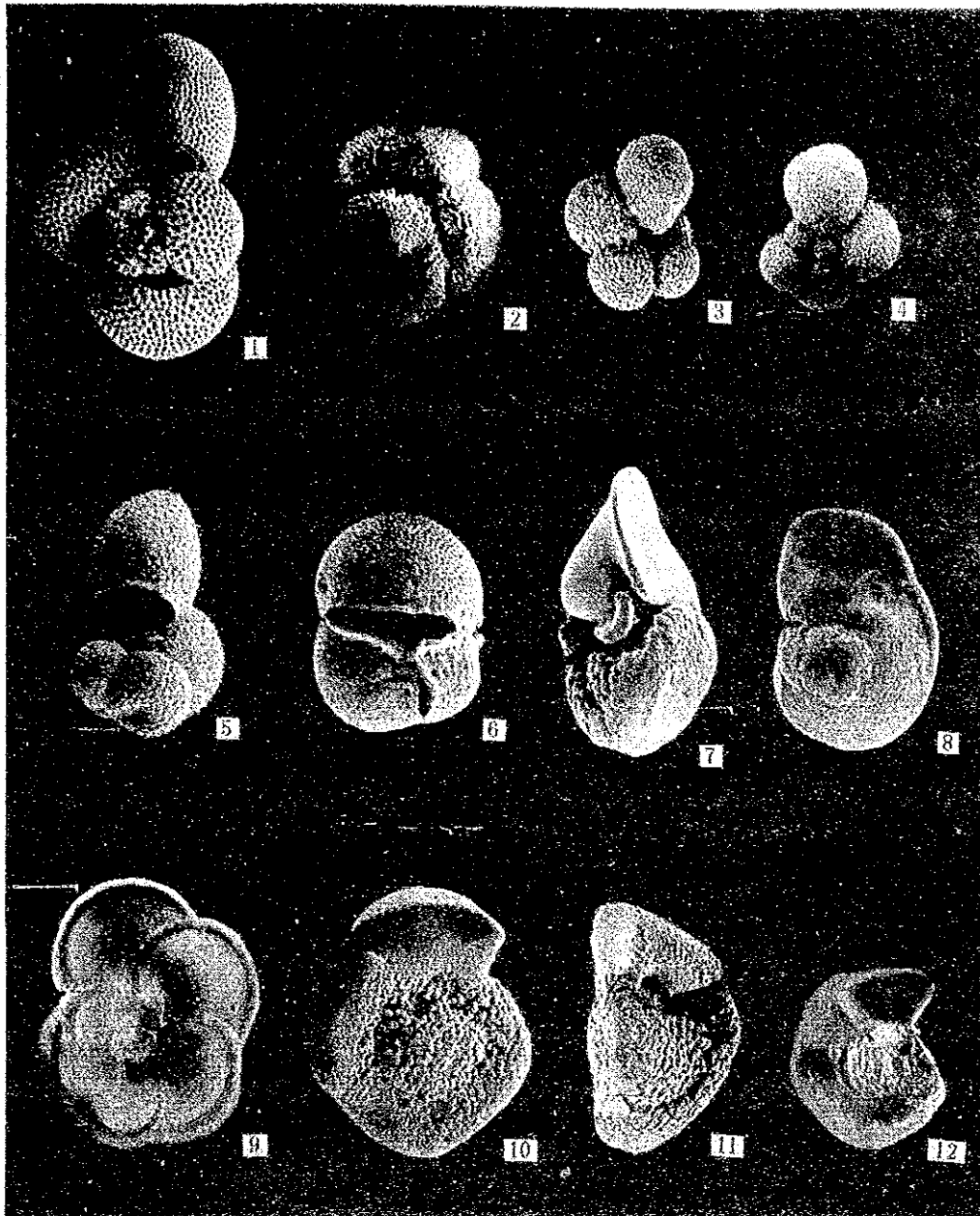
88S0975SC01 (Nos. 1~3)

Sample Nos. 1~3 do not contain planktonic foraminifera fossils and the geologic age cannot be determined.



- | | | |
|--|--------|--------|
| 1. <i>Reophax cf. nodulosus</i> Brady | No. 4 | x 54 |
| 2. <i>Haplophragmoides</i> sp. | No. 7 | x 54 |
| 3. <i>Recurvoides</i> sp. | No. 7 | x 54 |
| 4. <i>Ehrenbergina</i> sp. | No. 7 | x 54 |
| 5. <i>Epistominella exiqua</i> (Brady) | No. 7 | x 108 |
| 6. <i>Epistominella exiqua</i> (Brady) | No. 7 | x 108 |
| 7. <i>Cibicides pseudoungelianus</i> (Cushman) | No. 7 | x 54 |
| 8. <i>Cibicides</i> ? sp. | No. 7. | x 32.5 |
| 9. <i>Eponides bradyi</i> Earland | No. 7 | x 54 |
| 10. <i>Globocassidulina subglobosa</i> Brady | No. 8 | x 32.5 |
| 11. <i>Melonis pompilioides</i> (Fichtel & Moll) | No. 7 | x 54 |

Figure 3-3-6 Species of the Typical Foraminifera Fossils (1)



- | | | | |
|-----|---|-------|--------|
| 1. | <i>Globigerinoides sacculifer</i> (Brady) | No. 9 | x 54 |
| 2. | <i>Globigerinoides conglobatus</i> (Brady) | No. 7 | x 32.5 |
| 3. | <i>Globigerinella calida</i> (Parker) | No. 9 | x 54 |
| 4. | <i>Globigerinella calida</i> (Parker) | No. 9 | x 54 |
| 5. | <i>Beella digitata</i> (Brady) | No. 9 | x 54 |
| 6. | <i>Sphaeroidinella dehiscens</i> (Parker & Jones) | No. 8 | x 32.5 |
| 7. | <i>Globorotalia tumida</i> (Brady) | No. 9 | x 32.5 |
| 8. | <i>Globorotalia tumida</i> (Brady) | No. 9 | x 32.5 |
| 9. | <i>Globorotalia menardii</i> (Parker, Jones & Brady) | No. 8 | x 32.5 |
| 10. | <i>Globorotalia crassaformis</i> (Galloway & Wissler) | No. 8 | x 54 |
| 11. | <i>Globorotalia crassaformis</i> (Galloway & Wissler) | No. 8 | x 54 |
| 12. | <i>Globorotalia truncatulinoides</i> (d'Orbigny) | No. 9 | x 32.5 |

Figure 3-3-6 Species of the Typical Foraminifera Fossils (2)

88S0879SC01 (Nos. 4~6)

These samples do not contain planktonic foraminifera and the age is unknown.

88S1179SC01 (Nos. 7~9)

Globorotalia truncatolinoides, *Beella digitata* and *Globigerinella calida* occur in sample Nos. 7~9, these are post Pleistocene (N22-23) sediments. The fact that *Globigerinoides fistulosus*, and *Globorotalia tosaensis* do not occur and that *Pulleniatina oblicuiolculata* is dextral indicate the possibility of after Middle Pleistocene age (Ikebe and Tsuchi ed., 1984).

iv) Sedimentary environment

88S0975SC01 (Nos. 1~3)

There are no calcareous foraminifera in these samples and population consisting only of agglutinate species indicate formation in environment deeper than CCD. The CCD in equatorial waters is approximately 5,000 m.

88S0879SC01 (Nos. 4~6)

There are no calcareous foraminifera in these samples and population consisting only of agglutinate species indicate formation in environment deeper than CCD.

88S1179SC01 (Nos. 7~9)

These samples contain population with large proportion of *E. exiqua*, *E. umboniferus*, deep sea species. This indicates formation in environment shallower than CCD.

v) Sedimentation rate

88S0975SC01 (Nos. 1~3)

The rate of sedimentation could not be calculated by foraminifera as age determination was not possible.

88S0879SC01 (Nos. 4~6)

The rate of sedimentation could not be calculated by foraminifera as age determination was not possible.

88S1179SC01 (Nos. 7~9)

These are sediments formed during Pleistocene (N22-23) or later. they were formed, thus, later than 1.8 Ma and if the sedimentation occurred continuously and is reflected in the samples, the rate of sedimentation is calculated to be "depth of sample No. 9/1.8 million years<".

3-4 MFES Survey of Manganese Nodules

1) Effect of topography and sediments.

A scatter diagram of the sampling data and the MFES survey results are shown in Fig. 3-4-1 (1), (2). The diagram shows the following results.

i) Types c, d₂ zones

In the survey area, these types occur almost solely in the flat sea-floor and the hard bedrock shows high reflectivity and forms false anomalous zones. Therefore, the c, d₂ zone should be deleted when considering the manganese nodule abundance from MFES data. From past experience, the manganese nodule potential of the c, d₂ zone is low, and is often barren.

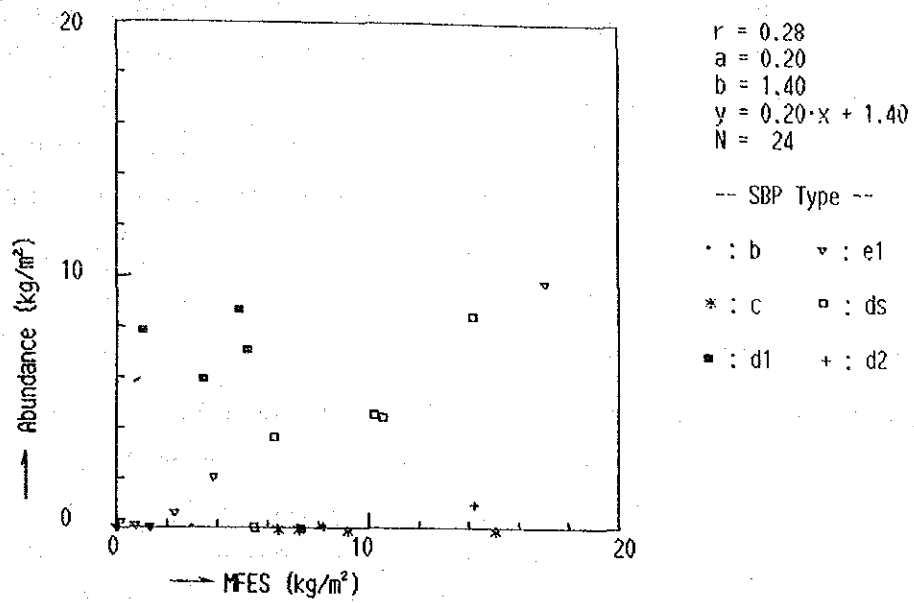
ii) Type d₁ zones

False anomalies are not rare in the mountainous and knoll provinces, also normal reflection energy is not obtained from steep and complex topography. Therefore, as observed from the scatter diagram, MFES values are often lower than the sampled results. Thus from reasons opposite to (i), mountainous and knoll zone should also be deleted.

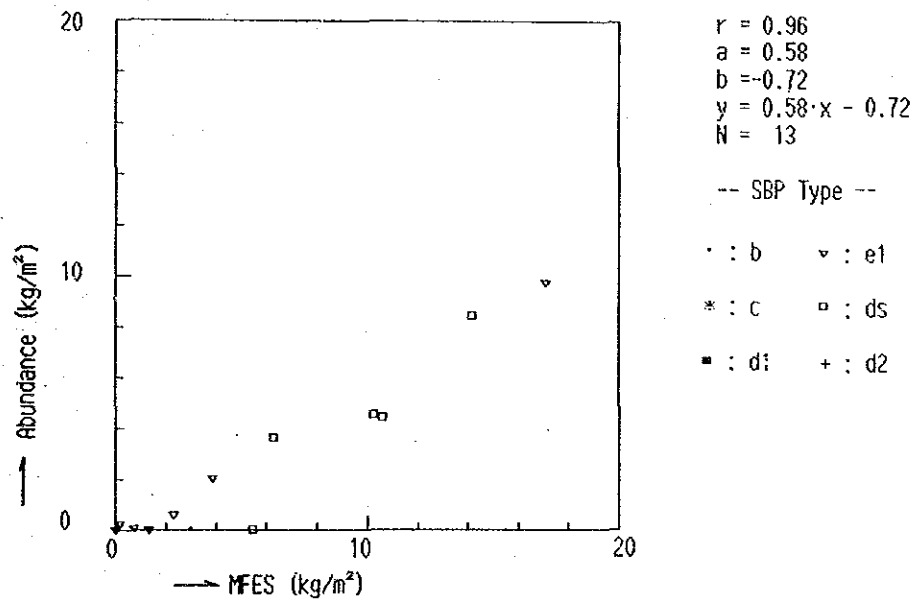
iii) Type d_s zone

The correlation between MFES data and the sampling results in the type d_s areas, is good in the scatter diagram. Generally, however, the areas of type d_s distribution have high relief and the reliability of measurements is often not high due to echos and scattered reflection. Because of this, type d₂ area was deleted from the manganese nodule abundance maps together with (ii) and (iii) areas in our previous investigations. In the present survey area, this zone cannot be ignored because of the good correlation in the scatter diagram.*1

*1 The small number of data could have resulted in better-than-real apparent correlation.



(1) Whole survey stations



(2) Excluding type d1,d2 and c

Figure 3-4-1 Relation Between MFES Intensity and Abundance of Manganese Nodules

iv) Type e₁ zone

Upper transparent layer exist in this type, the reliability of MFES values is generally high and the correlation with the manganese nodule distribution is good. The scatter diagram is not very clear because of the small number of data, but the correlation is good. Also in some track lines of this survey area. Type b with upper transparent layer is observed, this has characteristics similar to e₁.

2) Buried Manganese Nodules

The distribution of buried manganese nodules in this survey area is shown in Fig. 3-4-2. It is seen that almost all of the manganese nodules in this area belong to the buried type*1. The result of our study on the effect of the buried type is shown in Fig. 3-4-3. The solid circles of this figure are the buried type with buried ratio higher than 0.4, and the open circles indicate those considered to be exposed. In the scatter diagram, both types are plotted on the same regression line and the effect of buried type is inferred to be nil. In other words, both types of manganese nodules can be detected by MFES.

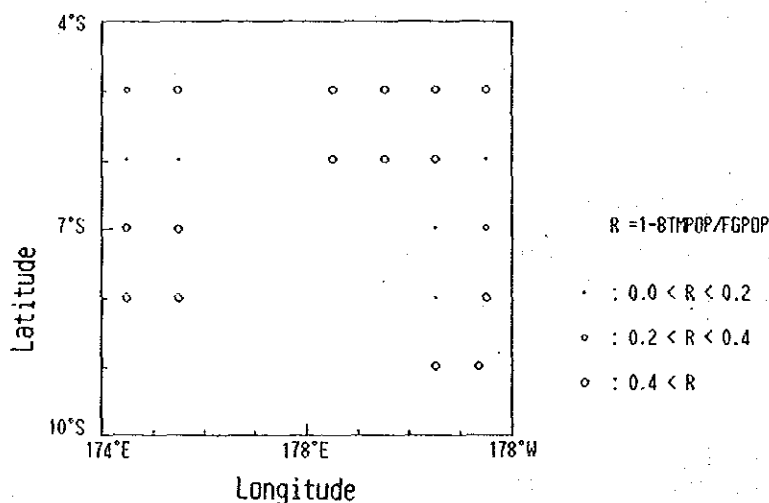


Figure 3-4-2 Distribution of Embedded Type Manganese Nodules

*1 In this section, the definition of buried type is $(1 - \text{BTMPOP} / \text{FGPOP}) > 0.4$

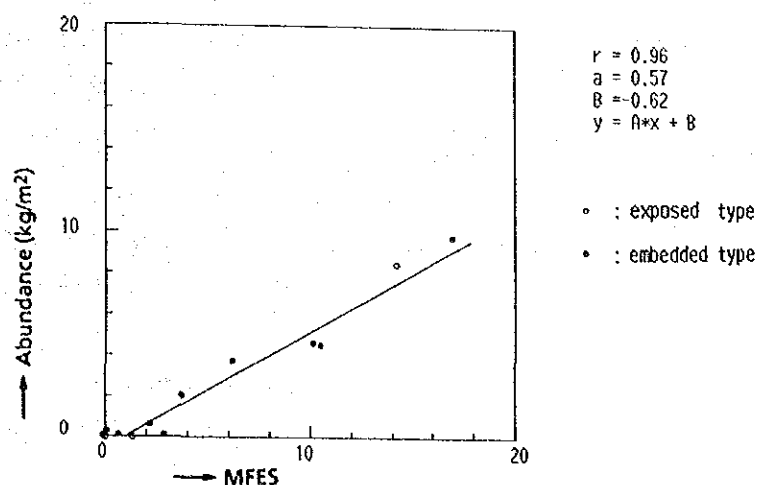


Figure 3-4-3 Influence of Embedded Type Manganese Nodules on MFES Measurement

3) Estimation of Manganese Nodule Distribution by MFES

Based on the results of work reported in the previous sections, a figure was drawn incorporating the analysis of the MFES values and SBP types (Annexed Fig. 6). The distribution of various SBP types, namely d₁ indicating seamounts, knolls and their vicinity; c, d₂ inferred to be barren; and also d_s inferred to have low reliability of data, as well as the results of sampling are shown in this figure. The distribution of these types are as follows.

[Plains]

North of approximately 6°30'S, c, d₂ indicating opaque upper layers are distributed and the zone is inferred to be barren. On the other hand, e₁ indicating transparent upper layers are widely distributed to the south of the above. Here, the reliability of MFES is high, and the zone, with the exception of the knolls, is a low abundance zone of 0~2.5 kg/m². Thus, this entire flat zone is concluded to be a very low manganese nodule field.

[Mountainous zone]

The sea-floor between the seamounts is relatively flat and is predominantly of type c. Only very small parts have upper transparent layers. The abundance is low at 0~0.25 kg/m². Similar to (1), this zone is predominantly c, d₂ zone and is inferred to be barren.

[Quasi plains]

This is a predominantly type d₁ and d_s province, and the topography has clear and rich relief. The zones where MFES is applicable is the flat zone in the north of 5°S and the vicinity of some seamounts and knolls, these zones are in variably of low abundance 0~5 kg/m².

They are localities which have higher than 10 kg/m² but the extent is very small. Also there are sporadic localities of higher than 7.5~10 kg/m² abundance in type d_s zone.

These are zones of low MFES reliability and further investigation is necessary to confirm the abundance.

3-5 Modes of Manganese Nodule Occurrence

1) Classification and Properties

The modes of occurrence of manganese nodules are analysed in the view of their morphology, size and external appearance and the characteristics of the distribution are explained.

Manganese nodules are classified mainly by their morphology as shown in Fig. 3-5-1 (1)-(2).

The physical properties are summarised in Table 3-5-1. The ratio of each type in sampled nodules is shown in Fig. 3-5-2.

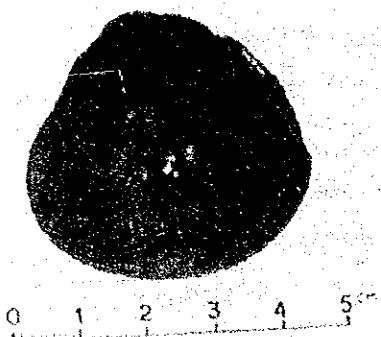
(1) Morphology

Manganese nodules are divided into the following seven types.

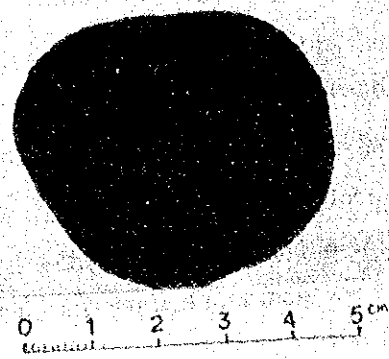
- | | |
|-----------------------|--|
| Spheroidal type: | Nearly perfect sphere. |
| Ellipsoidal type: | Hamburger-shaped external form and crushed spheroidal form. |
| Ellipsoidal fat type: | More irregular and larger than ellipsoidal type. |
| Pebble type: | Beach and river gravel shape (diameter around 23~4 cm). |
| Pebble type: | This type looks like gravel on shore and on the river bed. Its diameter is around 2~4 cm. |
| Massive type: | Irregular and angular shape (including various shapes such as spheroidal, ellipsoidal or plate). |
| Plate type: | Thin and round shape like roof shingles or rice cakes. |
| Other type: | The manganese nodules which cannot be classified into the above six types. |

[Spheroidal type]

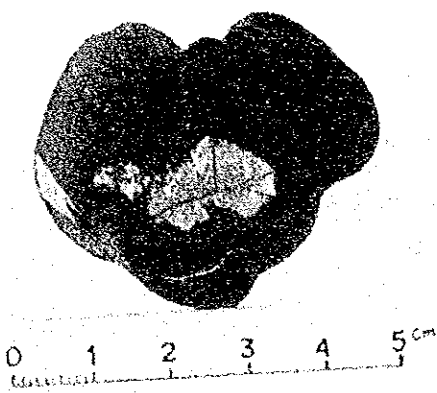
The diameter is mostly between 1~5 cm with a maximum of about 8cm. Manganese nodules larger than 2 cm in diameter have various surfaces such as slightly smooth or rough. Smooth surface is more common. On the other hand, manganese nodules smaller than 2 cm in diameter have round shaped projections and are mainly like the candy confetto with rough surface.



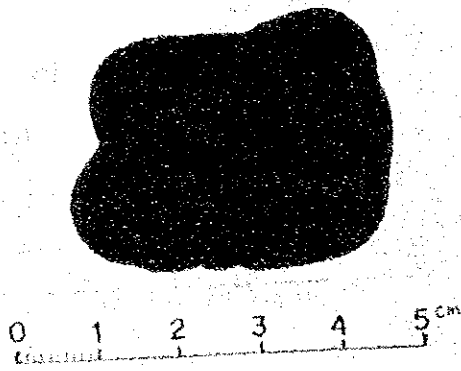
88S0674FG03 (Section)
Spheroidal



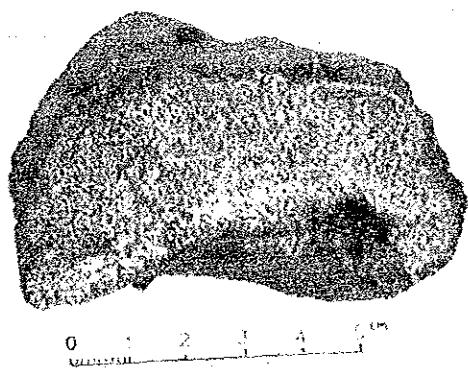
(Upper surface)



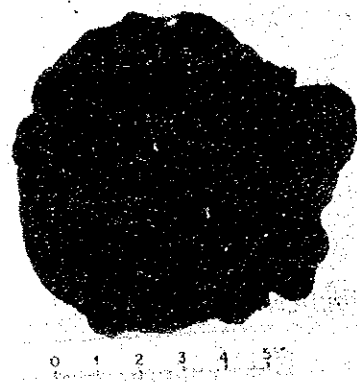
88S0874FG01 (Section)
Massive



(Upper surface)

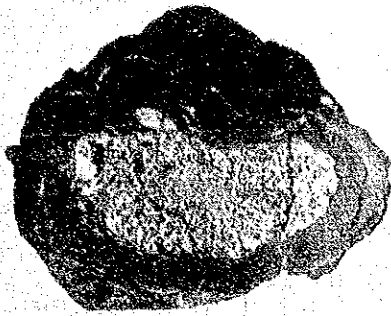


88S0679FG01 (Section)
Ellipthoidal

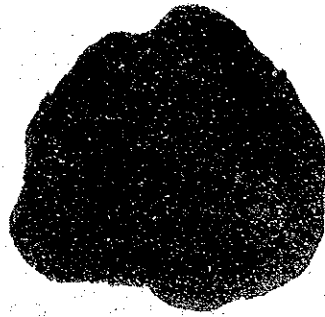


(Upper surface)

Figure 3-5-1 Morphology of Manganese Nodules (1)



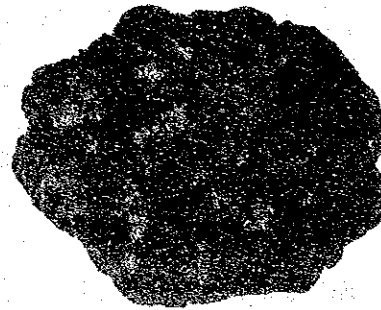
88S0780FG03 (Section)
Ellipthoidal Fat



(Upper surface)



88S0879FG02 (Section)
Ellipthoidal Fat



(Upper surface)



88S0679FG01 (Upper surface)
Other



88S0674FG03 (Upper surface)
Other

Figure 3-5-1 Morphology of Manganese Nodules (2)

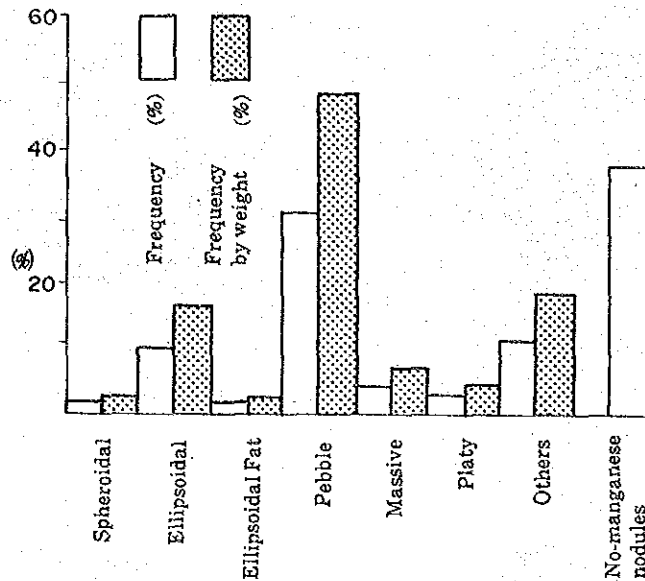


Figure 3-5-2 Morphology and Sampling Weight of Manganese Nodules

[Ellipsoidal type]

The surface is rough and irregular and rarely has cracks. It constitutes about 16% of the manganese nodules of the area.

[Ellipsoidal fat type]

This type is one of the variations of the ellipsoidal type and is larger than the former type. In this survey area, this type was observed rarely.

[Pebble type]

These are pebble to semi-breccia and the diameter is mostly between 2~4 cm. The surface is smoother than the other types. The combined type manganese nodules are more abundant compared with the other types. It constitutes 49% of the manganese nodules of the area.

[Massive type]

The diameter is mostly between 4~6 cm. The larger sized ones have hardly any angular shape and shows "potato" shape. Many have irregular shape. The surface is mostly rather smooth.

[Plate type]

The size varies. The surface is mainly smooth and contains rock fragments inside.

[Other type]

In the surveyed area, most of the manganese nodules classified into this type are so small (less than 5 mm) that these shapes are difficult to be determined. The stick shaped are also grouped in this type.

(2) Size distribution

The size distribution of manganese nodules is shown in Fig. 3-5-3. This figure indicates that the medium-sized manganese nodules with 2~6 cm in diameter are the most common, constituting 75% of the nodules in this area.

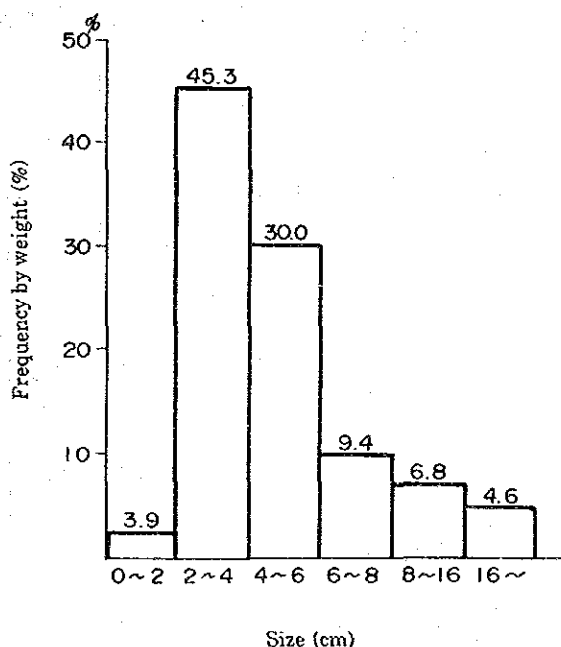


Figure 3-5-3 Size and Sampling Weight of Manganese Nodules

(3) Characteristics of external appearance

The characteristics of external appearance are shown in Table 3-5-1. The surface of the manganese nodules vary from relatively rough (R-type) to smooth (S-type). Most of the manganese nodules in the surveyed area are classified into "S-type". This tendency is constant throughout the area.

Table 3-5-1 Physical Properties Associated with Morphology of Manganese Nodules

		Spheroidal	Ellipsoidal	Ellipsoidal fat	Pebble	Massive	Platy	Others
Size (cm)	0 ~ 2							
	2 ~ 4							
	4 ~ 6							
	6 ~ 8							
	8 ~ 16							
Surface texture	Smooth							
	Smooth > Rough							
	Smooth < Rough							
	Rough							
Single/Poly	Smooth							
	Smooth > Rough							
	Smooth < Rough							
	Rough							
Crack	Single type							
	Single > Poly							
	Single = Poly							
	Single < Poly							
Fissure	Poly type							
	Many							
	Medium							
Moisture content (%)	Rare							
	Mean	27.81	30.58	26.89	26.88	24.57	27.59	22.90
	Standard deviation	2.18	0.00	3.16	0.58	3.12	1.93	0.69
Specific gravity (wet)	Maximum	31.72	30.77	32.21	27.92	30.00	30.73	23.81
	Minimum	15.38	30.43	20.00	26.59	19.29	23.91	22.40
	Mean	2.02	20.1	2.03	2.03	2.06	2.01	1.93
	Standard deviation	0.03	0.00	0.07	0.07	0.05	0.04	0.02
	Maximum	2.08	20.3	2.14	2.06	2.11	2.10	1.94
	Minimum	1.86	2.00	1.86	1.90	1.90	1.87	1.90